thematic review

Thematic Review Series: Lipids and Lipid Metabolism in the Eye

Retinal very long-chain PUFAs: new insights from studies on ELOVL4 protein

Martin-Paul Agbaga,*,†,§ Md Nawajes A. Mandal,†,§ and Robert E. Anderson[1],*,†,§

Departments of Cell Biology* and Ophthalmology,† University of Oklahoma Health Sciences Center, and Dean A. McGee Eye Institute,§ Oklahoma City, OK 73104

Abstract Compared with other mammalian tissues, retina is highly enriched in PUFA. Long-chain PUFA (LC-PUFA; C18-C24) are essential FAs that are enriched in the retina and are necessary for maintenance of normal retinal development and function. The retina, brain, and sperm also contain very LC-PUFA (VLC-PUFA; >C24). Although VLC-PUFA were discovered more than two decades ago, very little is known about their biosynthesis and functional roles in the retina. This is due mainly to intrinsic difficulties associated with working on these unusually long polyunsaturated hydrocarbon chains and their existence in small amounts. Recent studies on the FA elongase elongation of very long chain fatty acids-4 (ELOVL4) protein, however, suggest that VLC-PUFA probably play some uniquely important roles in the retina as well as the other tissues. Mutations in the *ELOVL4* gene are found in patients with autosomal dominant Stargardt disease. Here, we review the recent literature on VLC-PUFA with special emphasis on the elongases responsible for their synthesis. We focus on a novel elongase, ELOVL4, involved in the synthesis of VLC-PUFA, and the importance of these FAs in maintaining the structural and functional integrity of retinal photoreceptors.—Agbaga, M-P., M. N. A. Mandal, and R. E. Anderson. **Retinal very long-chain polyunsaturated fatty acids: new insights from studies on ELOVL4 protein. *J. Lipid Res.* 2010.** 51: **1624–1642.**

Supplementary key words very long-chain saturated fatty acids • retinal lipids • Stargardt Disease

Very long-chain FA (VLC-FA) are components of cellular lipids that contain hydrocarbon chains ranging from C26 to C40 either as saturated and monounsaturated FAs or as PUFA. Although VLC-FA and VLC-PUFA are relatively rare compared with the abundance of FA containing 16–22 carbons, they are widely distributed in higher plants and animals (1–10). They are found in most living organisms from humans to autotrophic and heterotrophic lower organisms, including microalgae, sponges, bacteria, and fungi (1, 9, 11–15). VLC-FA are found mainly in seed oils, plant waxes, cutin, suberin, skin, hair, and wax glands (1), whereas VLC-PUFA are found primarily in retina, brain (1, 16), testis, and spermatozoa (17–19).

The unusually long hydrocarbon chains with 3–9 double bonds, which are prone to oxidative damage, combined with the small quantities found in mammalian tissues, have made them difficult to isolate and analyze in detail over the years (9). Very little is therefore known about the metabolism and function of VLC-PUFA and VLC-FA in mammals, except for their increase in disorders of peroxisomal function (3, 16, 20, 21), as components of the secretions of meibomian glands (22–27), and their reduction in animal models of autosomal dominant Stargardt-like macular dystrophy (STGD3) (28–32), a juvenile form of macular degeneration. In contrast, the roles of long-chain PUFA (LC-PUFA) with carbon chains that range from C18 to C24 are fairly well understood, especially in the retina and other neural tissues. A detailed account on the role and function of LC-PUFA in the retina was reviewed earlier (33–36).

Recent interest in the molecular and physiological roles of VLC-PUFA in the retina came from the finding that the gene associated with STGD3 shared sequence homologies with genes involved in FA elongation (37, 38). The gene

This work was supported by the following National Institutes of Health Grants: EY00871, EY04149, EY12190, and RR17703; and by the Foundation for Fighting Blindness, Research to Prevent Blindness, and Hope for Vision. Its contents are solely the responsibility of the authors and do not necessarily represent the official views of the National Institutes of Health or other granting agencies.

Manuscript received 21 December 2009 and in revised form 18 March 2010.

Published, JLR Papers in Press, March 18, 2010
DOI 10.1194/jlr.R005025

Abbreviations: AOX, acyl-CoA oxidase; DHA or 22:6n3, docosahexaenoic acid; ELOVL, elongation of very long-chain FA; ELOVL4, elongation of very long-chain FA-4; ERG, electroretinogram; LC-PUFA, long-chain PUFA; PC, phosphatidylcholine; ROS, retinal outer segments; RPE, retinal pigment epithelium; STGD1, recessive Stargardt degeneration; STGD3, autosomal dominant Stargardt-like macular dystrophy; VLC-FA, very long-chain saturated or monounsaturated FA; VLC-PUFA, very long-chain PUFA.

[1]To whom correspondence should be addressed.
e-mail: robert-anderson@ouhsc.edu

was named *Elongation of Very Long Chain fatty acids-4* (*ELOVL4*). We identified the metabolic function of the ELOVL4 protein and showed that it is indeed a component of an elongase system involved in biosynthesis of VLC-PUFA (39).

This review will summarize our current knowledge of VLC-PUFA with respect to their distribution, biosynthesis, and possible function in the tissues in which they are found. We will focus much of our attention on the retina, which, apart from mammalian sperm, contains high levels of VLC-PUFA of any mammalian tissue, and on the novel elongase, ELOVL4, that is responsible for VLC-PUFA biosynthesis in retina, testes, and the brain.

NOMENCLATURE AND STRUCTURE OF VLC-FA AND VLC-PUFA

There has been very little change in nomenclature of FA over the years despite the advent of International Union of Pure and Applied Chemistry system of naming. For the most part, trivial names of the FA such as docosahexaenoic acid (DHA, or 22:6n3) or arachidonic acid (20:4n6) still prevail and are more commonly used (9). Also, because most studies done previously were focused on FA with a maximum of 22 carbons, most studies refer to FA such as 20:4n6, 22:5n3, and 22:6n3 as either LC-PUFA or VLC-PUFA (3, 9, 21, 40, 41). With advancement in science and technology, coupled with improvement in analytical methods for detection, identification and quantification of FA with carbons chain longer than C22 by GC-MS and/or LC/ESI-MS and LC-MS/APCI, among others, we are now in a new era of beginning to appreciate the presence and possible function of FA with carbon chains longer than C22 (42). As such, we suggest that there is the need to regroup and redefine some of these FA based on our current knowledge. For this review, we define VLC-FA as saturated and monounsaturated FAs with C26–C40 or more carbon chains. These may exist as even- or odd-numbered, straight- or branched-chain, hydroxylated or nonhydroxylated FAs (3, 9, 11). We further define VLC-PUFA as PUFA containing an even or odd number of carbons from C26 to C40 or more with 3-9 *cis* (*Z*) double bonds (3, 10–12). Previous publications have described some of these FA as extremely LC-PUFA (43–45) or ultra-long-chain FAs (21). We define the C18–C24 PUFA with 3–7 double bonds in the *cis* (*Z*) conformation as LC-PUFA (10).

The VLC-PUFA found in tissues are unique in that the proximal carboxylic region is composed of 12–20 saturated carbon bonds, whereas the distal region (CH_3 group end) contains 5 or more methylene interrupted *cis* double bonds, as shown in **Fig. 1A–**C. Positions of the *cis* (Z) double bonds are numbered from the COOH group. By their unique structure, these FA have the length to occupy both halves of a lipid bilayer or be associated with proteins within one half of the bilayer and give quite different biophysical properties to each domain.

Both VLC-FA and VLC-PUFA rarely exist as free FA (Fig. 1A, B) in tissues; instead, their carboxyl head groups are usually esterified to glycerol to form glycerolipids or modified through an amide bond linkage to form sphingolipids or ceramides. As glycerolipids, they may be esterified to either the *sn-1* or *sn-2* position of the glycerol backbone, which in turn can be modified by the addition of polar head groups to the *sn-3* position to form different phospholipids (Fig. 1C).

DISTRIBUTION, ABUNDANCE, AND BIOSYNTHESIS OF VLC-PUFA

Over 20 years ago, Aveldano and Sprecher (4, 6) reported the existence in the vertebrate retina of unusually LC-PUFA with carbon chains ranging from C26–C36. They showed that these unique and novel retinal FA occur as a dipolyunsaturated molecular species of PC, with 22:6n3 as the predominant partner. The retinal outer segment (ROS) membranes were highly enriched in PC-containing VLC-PUFA (1, 2). Later, Poulos et al. (16) confirmed the existence of 22:6n3, 32:6n3, and 34:6n3 as major components of the PC fraction obtained from the bovine retina. Although these FA usually constitute <2% of total retinal lipids, the PC-containing VLC-PUFA compose 13% of the PC fraction of retinal ROS membranes (3, 4).

The presence of VLC-PUFA in the mammalian testis was first reported in the late 1960s (46–50). Later, Grogan et al. (51, 52) reported that isolated spermatocytes and spermatids synthesized VLC-PUFA from ^{14}C-acetate or [1-^{14}C]20:4n6. Also, cells from later stages of spermatogenesis elongated [1-^{14}C]20:4n6 precursor to [^{14}C]22:4n6, [^{14}C]22:5n6, [^{14}C]24:4n6, and [^{14}C]24:5n6. The synthesized LC-PUFA were primarily esterified in the *sn-3* position of the glycerol backbone of triacylglycerols. When rat testes were injected with [1-^{14}C]20:4n6, the spermatids contained [^{14}C]26:4, [^{14}C]26:5, [^{14}C]28:5, and [^{14}C]30:5 (53). Similar studies done in the seminiferous tubules showed active desaturation of 24:4n6 to 24:5n6 and concomitant formation of odd- and even-chain tetraenoic and pentaenoic FA up to C32 (17). Ram, boar, bull, and human spermatozoa also contain both odd-chain (for ram and boar) and even-chain VLC-PUFA (C26–C38) (54). Interestingly, most of the testis- and spermatozoa-related VLC-PUFA are amide bound in sphingomyelin and ceramides instead of ester bound in phosphatidylcholine (PC), as found in the retina (18, 19, 55).

Triacylglycerols and cholesterol esters containing VLC-PUFA were also found in rat testes and sperm (17). In rat testes, 28:4n6 and 30:5n6 constitute the most abundant VLC-PUFA found in ceramides and sphingolipids (19). The VLC-PUFA content increased with the onset of spermatogenesis, reaching almost 15% and 40% of the total FA in sphingomyelin and ceramides, respectively. As in the retina, these FA, together with 22:6n3, remain at high levels during adult life in fertile rats and then decrease during older age (19, 56).

Studies on bull and ram spermatozoa found VLC-PUFA in sphingomyelin and ceramide. The VLC-PUFA content reached almost 70% in the sphingomyelin of freshly harvested spermatozoa from adult bull, while ram spermato-

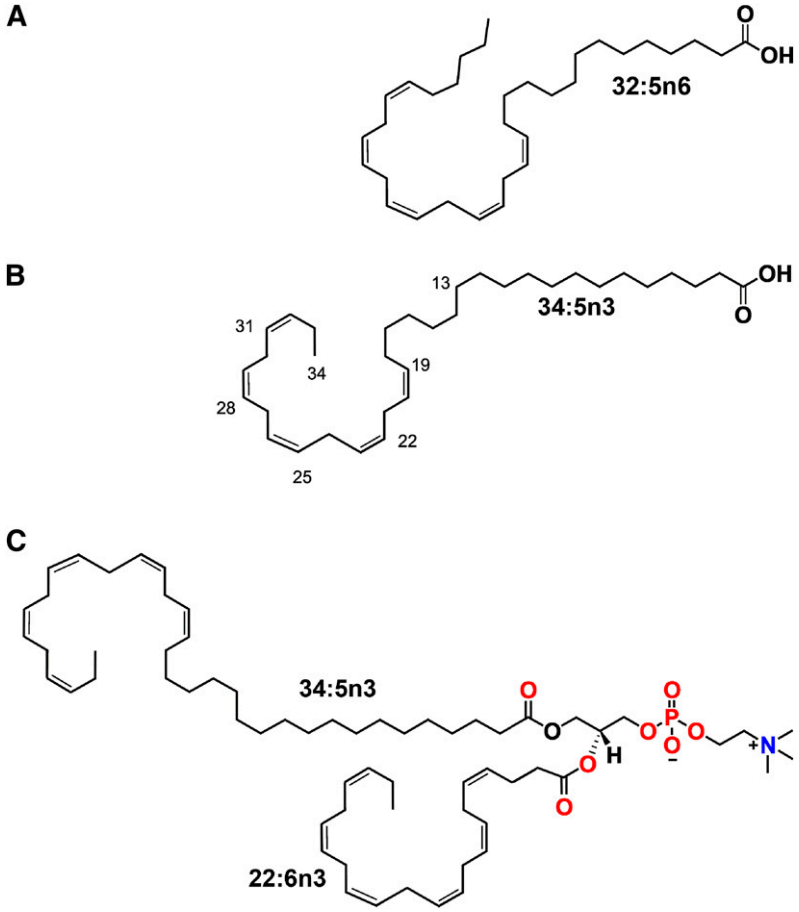

Fig. 1. Structure of VLC-PUFA. Free FA form of VLC-PUFA 32:5n6 (A) and 34:5n3 (B). Note the polyunsaturated methyl end and the saturated carboxyl terminal ends. C: A typical phospholipid containing VLC-PUFA esterified to the *sn-1* position of the glycerol backbone. LC-PUFA, either 22:6n3 or 20:4n6, or others can occupy the *sn-2* position. The *sn-3* position in this scenario is occupied by phosphocholine.

zoa contained even higher concentrations of VLC-PUFA in both sphingomyelin and ceramides (18). The predominant FA in the sphingomyelin and ceramides include 32:6n3, 30:6n3, and 34:6n3. Sphingomyelin accounted for 13–15% of the total phospholipids in bull and ram spermatozoa; thus, the 70–80% VLC-PUFA in sphingomyelin represents a significant proportion of the total FA of bull sperm cells (18). The percentage of VLC-PUFA in sphingomyelin in sperm heads was significantly higher than in sphingomyelin of sperm tail fractions of both bulls and rats (18). Human spermatozoa differs from the other mammalian spermatozoa in that it contains up to C32 VLC-PUFA with 2–4 double bonds, whereas boar, ram, and bull spermatozoa contain 5 and/or 6 double bonds with chains up to 34 carbons (54). While n6 VLC-PUFA are most abundant in human and boar spermatozoa, ram and bull spermatozoa contain both n3 and n6 FA (54, 55). The presence of sphingomyelin containing unusual 2-hydroxylated and nonhydroxylated n6 VLC-PUFA with four to five double bonds has also been reported for boar and rat testes and spermatozoa (57).

In the brain as in the retina, VLC-PUFA are esterified at the *sn-1* position of the glycerol backbone of PC, with saturated, monounsaturated, and LC-PUFA molecules occupying the *sn-2* position (16, 58). They are also present in neutral lipids, predominantly in cholesterol esters, with smaller amounts in the nonesterified FA and triacylglycerols (59). The monounsaturated FA in the brain are mainly n7 and n9 isomers with the double bond in the *cis* configuration (3, 60, 61). The concentration of C24–C38 VLC-PUFA in brain sphingomyelin increases during development. Significant amounts of 34:4n6 and 36:4n6 have been found in rat brains (62), although 22:6n3, 24:4n6, and 24:6n3 are the most abundant PUFA. The healthy human brain also contains C30–C38 n6, with 34:4n6 and 34:5n6 as the major VLC-PUFA (63). Developmental and age-dependent changes in composition and concentration of these FA occur in both rat and human brains. VLC-PUFA exist at relatively higher concentrations in the brains of young rats and humans, in which 34:4n6 and 34:5n6 predominate, but are replaced with 36:4n6 in the adult (3, 63). Glycerophospholipids containing C28–C32 saturated and monounsaturated FA as well as cerebrosides and sulfatides containing VLC-FA have been found in the bovine brain (64, 65). Age-dependent increases in both saturated and monounsaturated C24–C28, including 25:0 and 25:1, have been found in cerebrosides, gangliosides, sphingomyelin, and total FA in the developing rabbit brain (66). These developmental changes have been suggested to be due to specific incorporation of these FA into myelin lipids (66). Neonatal rat brains are capable of elongating and desaturating [1-^{14}C] 26:4n6 to C28–C36 tetraenoic and C26–C38 pentaenoic VLC-PUFA that can undergo peroxisomal β-oxidation (58).

Poulos and Sharp (16, 20, 59, 67) reported the presence of VLC-PUFA of C26–C38 in the brains of patients with the cerebro-hepato-renal (Zellweger) syndrome. Zellweger syndrome

is a rare and fatal autosomal recessive inherited disorder characterized ultrastructurally by the marked deficiency of peroxisomes and biochemically by the reduction of 22:6n3 and the accumulation of VLC-PUFA in the brain (16, 20, 59, 67), plasma, and cultured fibroblasts from the skin of these patients (68). Other peroxisomal disorders are also associated with an increase in VLC-FA and VLC-PUFA in brain and plasma (69–77). Postmortem analyses of 4 day- to 5 month-old whole brains of Zellweger patients showed higher concentrations of VLC-PUFA than those found in normal brains (16). The predominant VLC-PUFA in Zellweger brains contains five and six double bonds, whereas C32–C38 VLC-PUFA with four and five double bonds are the major FA in normal brains (16). Zellweger brains had trace amounts of C40 VLC-PUFA of the n6 family, which were not found in normal brains (16). The presence of elevated levels of VLC-FA and VLC-PUFA in specific ratios (mostly 28:5/22:0) is used as one of the bases of diagnosis of the disease (1, 59). Interestingly, the levels of 22:6n3 are drastically reduced in peroxisomal disorders, reflecting its synthesis in the peroxisomes.

Recently, a knockout mouse model of human straight-chain acyl-CoA oxidase (AOX) deficiency (pseudo-neonatal adrenoleukodystrophy) was generated (44, 78, 79). AOX is a peroxisomal enzyme that is regulated by peroxisome proliferator activated receptor-α (80, 81) and catalyzes the rate-limiting step in peroxisomal β-oxidation of saturated and polyunsaturated FA with 22 or more carbons (44, 80, 81). The livers of weanling $AOX^{-/-}$ mice had already accumulated n3 and n6 LC-PUFA and VLC-PUFA (C24–C30) with five to six double bonds (44). The n3 FA were 22:5n3, 24:6n3, 26:6n3, and 28:6n3, whereas 22:4n6, 22:5n6, 24:5n6, 26:5n6, and 28:5n6 were the major n6 PUFA (44). Compared with controls, these animals also had an increase in 26:0 in their plasma (44, 78, 79). When injected intraperitoneally with [U-^{13}C]18:3n3, there was greater incorporation of [U-^{13}C]18:3n3 into 24:6n3, 26:6n3, and 28:6n3 in the liver of $AOX^{-/-}$ mice than in controls. While the accumulation of VLC-PUFA in these mice underlies the functional role of AOX in β-oxidation of LC/VLC-PUFA and VLC-FA, it also suggests that these lipids are probably normal cellular lipids that may be metabolized through the peroxisomal β-oxidation pathway.

The presence of 28:7n3 and 28:7n6 has been identified in Baltic herring (*Clupea harengus*), while 28:7n6 and 28:3n3 have also been found in several species of marine dinoflagellates in which VLC-PUFA accounted for <2.3% of the total FA (11, 12). For example, 28:8n3 has been reported in commercial fish oil concentrates (9). FA with 34 carbons and containing nine double bonds (all in the *cis* or Z configuration) have also been reported in the freshwater crustacean, *Bathylnella natans* (10). The tetratriacontanonaenoic acid (34:9n6) is found in diacyl PC, with 16:0, 18:0, and 16:1 as the other acyl chains (10). Presence of mycolic acid (complex VLC-FA containing FA with diverse functional groups and branched-chain hydroxylated C28–C90 saturated or monounsaturated double bonds) in cell envelope of Mycobacterium such as *Mycobacterium tuberculosis*, promotes survival and resistance of the bacteria to the hosts' immune system and to antibiotic treatment regimes (9, 82).

In the eye, saturated and monounsaturated VLC-FA are found in meibomian glands and their secreted meibum as well as in secretions from Harderian glands (1, 3, 83–87). The FA in steer and human meibum contain a group of long-chain α and omega-diols (containing two hydroxyl groups) (88, 89). The omega-hydroxyl acids constituted 85% of straight-chain monounsaturated FAs, while 13% were branched-chain saturated and the remainder were branched-chain monounsaturated FAs (88). The major FA in meibomian gland secretions are mostly saturated and monounsaturated, with only trace amounts of VLC-PUFA (88). The absence of VLC-PUFA in such secretions that are exposed to the environment and the damaging effects of the UV rays from the sun is not surprising, because the double bonds of VLC-PUFA are particularly susceptible to oxidative damage by environmental factors, singlet oxygen, and UV radiation (90–92). Thus, enhanced susceptibility of the double bonds in VLC-PUFA to oxidative damage may account for their exclusion from the skin and meibomian secretions that are in constant contact with the environment. While myelin and the meibomian and Harderian glands and their secretions are rich sources of saturated and monounsaturated VLC-FA, the retina has relatively higher levels of VLC-PUFA (3, 4, 6). For example, in cod retina, 32:6n3 alone accounted for 15% of the PC FA, and the LC-PUFA 22:6n3 is 65% of the total retinal FAs (4). Chicken, rat, rabbit, and bovine retinas have greater amounts of C26–C36 n3 and n6 VLC-PUFA than toad retina, which contains only 24:6n3 (4, 6). VLC-PUFA constitute about 2% of bovine total retinal FA and 13% of PC in bovine ROS membranes (4, 6). The first analysis of VLC-PUFA in human retina by Bernstein et al. (93), using GC-MS, found n3 and n6 C26–C34 VLC-PUFA containing four to six double bonds; our laboratory has recently confirmed their results (R.E. Anderson, unpublished observations).

The biosynthesis of LC-PUFA and VLC-PUFA has been demonstrated in testis, spermatocytes, spermatids, skin fibroblasts, human endothelial cells, retinoblastoma cells, and the retina (51–53, 74, 94, 95). The ability of the retina to synthesize VLC-PUFA was first reported by Rotstein et al. (5, 56, 96, 97), who used radiolabeled precursors of LC-PUFA and VLC-PUFA or radiolabeled acetate or glycerol to show that the retina has the metabolic machinery necessary for biosynthesis of both LC-PUFA and VLC-PUFA from short-chain precursors. When they incubated bovine retinas with [1-^{14}C] eicosatetraenoate (20:4n6), docosapentaenoate (22:5n3), or docosahexaenoate (22:6n3), there was efficient uptake and active esterification of these FA into different phospholipid classes (96, 97). The selectivity of uptake and esterification of the FA into the different phospholipids was 22:6 > 22:5 > 20:4 (97). The most active synthesis and turnover of PUFA were observed in the PC fraction of retinal phospholipids (97). Subcellular fractionation of the retinas showed that the highest proportion of incorporation into dipolyunsaturated PC was in the ROS; lesser amounts were found in the mitochondria, microsomes, and a postmicrosomal supernatant (97).

Using [1-^{14}C] acetate, Rotstein et al. (5) demonstrated that the greatest amount of label was incorporated in

24:5n3, 24:5n6, 26:5n3, 30:6n3, 32:5n3, and 32:6n3, most of which was associated with PC. Labeling of LC-PUFA (C20–C24) was much less than that of VLC-PUFA (1, 5). These results led to the conclusion that there is an active local synthesis of VLC-PUFA in retinal cells (1). As will be discussed later, we now know that the enzyme responsible for the condensation reaction in the synthesis of VLC-PUFA is expressed only in those cells that have VLC-PUFA. It is not expressed in the liver. So, unlike what occurs with 20:4n6 and 22:6n3, which are synthesized in the liver and transported to target tissues like the retina and brain, VLC-PUFA are most likely synthesized from available C20 and C22 PUFA precursors in the tissues in which they are found.

In a study to determine which LC-PUFA (C22–C24) is the primary precursor for VLC-PUFA biosynthesis in the retina, rats were fed a semisynthetic, nutritionally complete diet containing 20% (w/w) fat with 3% (w/w) 22:6n3 (98). After 6 weeks, [^{3}H]20:5n3 or [^{3}H]22:6n3 was injected into the vitreous cavity and the in vivo metabolism of the FA determined after 48 h. The incorporation of the labeled FA into VLC-PUFA differed between the two FA. While 90% of [^{3}H]22:6n3 remained as 22:6n3 in retinal phospholipids, [^{3}H]20:5n3 was elongated to pentaenoic and hexaenoic VLC-PUFAs containing up to C34 (98). This study confirmed previous findings showing that the retina contained elongase and desaturase enzymes capable of VLC-PUFA biosynthesis (5, 99, 100). It also demonstrated that the retina has the ability to synthesize VLC-PUFA in situ through successive elongation and desaturation of the essential FA 20:5n3 and 22:6n3. The authors concluded that 22:6n3 is an end-product of LC-PUFA biosynthesis and is not a preferred substrate for further elongation to VLC-PUFA (98, 101). However, an alternative explanation is that the injected radiolabeled 22:6n3 was diluted by a large endogenous pool of 22:6n3, which lowered its specific activity compared with that of 20:5n3, and resulted in a relatively small amount of radioactivity being incorporated into VLC-PUFA. In recent studies in our laboratory, human embryonic kidney cells and pheochromocytoma cells (PC12 cells) transduced with *ELOVL4* elongated 22:6n3 to VLC-PUFA, as it did 20:5n3 and 22:5n3 (39, 102).

THE ROLE OF FA ELONGASE COMPLEX IN VLC-FA AND VLC-PUFA BIOSYNTHESIS

In eukaryotes, saturated and monounsaturated C14–C18 FA are synthesized de novo by the cytosolic FA synthase complex (103), whereas C18 n3 and n6 essential FA must be obtained from the diet (104–114). Subsequent elongation and desaturation of these FA occur in the endoplasmic reticulum by a membrane-bound, multi-enzyme complex called the elongase complex and result in the accretion of VLC-FA, LC-PUFA, and VLC-PUFA (103, 104, 114–117). The fatty acyl-CoA chain elongation cycle mediated by the elongase complex involves the addition of two carbons from malonyl-CoA to an existing fatty acyl-CoA to form an acyl-CoA that is two carbons longer (103, 116, 117). The initial condensation reaction, which is the rate-limiting step in the elongation process, is catalyzed by enzymes called ELOVLs; there are currently seven known members of this family in mammals (ELOVL1–7).

All of the ELOVLs share similar characteristic features, which include the presence of multiple hydrophobic transmembrane domains, a histidine box motif, and endoplasmic reticulum targeting/retrieval signals (104, 118). They catalyze the condensation of malonyl-CoA with an acyl$_{(n)}$-CoA to form the intermediate product called β-ketoacyl-CoA (**Fig. 2**, step 1) (119). Reduction of the β-ketoacyl-CoA to β-hydroxyacyl-CoA is mediated by β-ketoacyl reductase in the presence of NAD(P)H (Fig. 2, step 2). Dehydration by β-hydroxyacyl-CoA dehydratase yields *trans*-2,3-acyl-CoA (Fig. 2, step 3), and subsequent reduction of the enoyl-CoA by enoyl-CoA reductase in the presence of NAD(P)H (Fig. 2, step 4) generates the elongated fatty acyl$_{(n+2)}$-CoA (114). Whether the elongated product is released for use elsewhere in the cell or is retained to undergo another round of elongation depends largely on the specific needs of the organism (117, 119–121). Many of the elongases found in cells have overlapping functions (124), and more than one may act on the same substrate.

While there are seven ELOVL proteins identified so far that have specific substrates (usually based on FA chain length), the three other enzymes involved in the elongation reaction appear to be the same (104, 115). Thus, tissues or cells that do not normally express a particular elongase can still produce predicted elongation products if an appropriate exogenous elongase is introduced in those tissues or cells through viral transduction (39, 123) or by transfection with plasmids (124, 125). Even in heterologous systems, when provided with the proper precursor, an elongase from a different species can use the other three endogenous enzymes and make the elongated FA products (116, 126, 127).

TISSUE DISTRIBUTION, SUBSTRATE SPECIFICITY, AND FUNCTION OF MAMMALIAN FA ELONGASES

The first elongase enzymes were identified in *Saccharomyces cerevisiae* and named ELO1, ELO2, and ELO3 (37, 128). ELO1 was the first FA elongase to be identified as a defective gene in *S. cerevisiae* mutants (128), which were not able to grow normally on FA shorter than palmitic acid (16:0). The defective *ELO1* gene was eventually cloned and found to encode a 310 amino acid protein that elongates C14–C16 FAs (38, 128, 129). *ELO2* and *ELO3* genes were later found in the yeast genome based on their similarity to the *ELO1* gene (37). The ELO2 protein elongates both saturated and monounsaturated FA up to C24 (37). ELO3 elongates a wider group of saturated and monounsaturated FA and is essential for the conversion of C24:0 to C26:0, which is necessary for sphingolipid biosynthesis (37, 122, 128, 130, 131). Although all three ELO proteins catalyze the first critical step of condensation in FA biosynthesis, each has different substrate specificities with resultant distinct chain length-specific end products (40, 115, 122).

Orthologs of the yeast *ELO* genes have been found in mammals. Mouse *Elovl3* was the first mammalian FA elon-

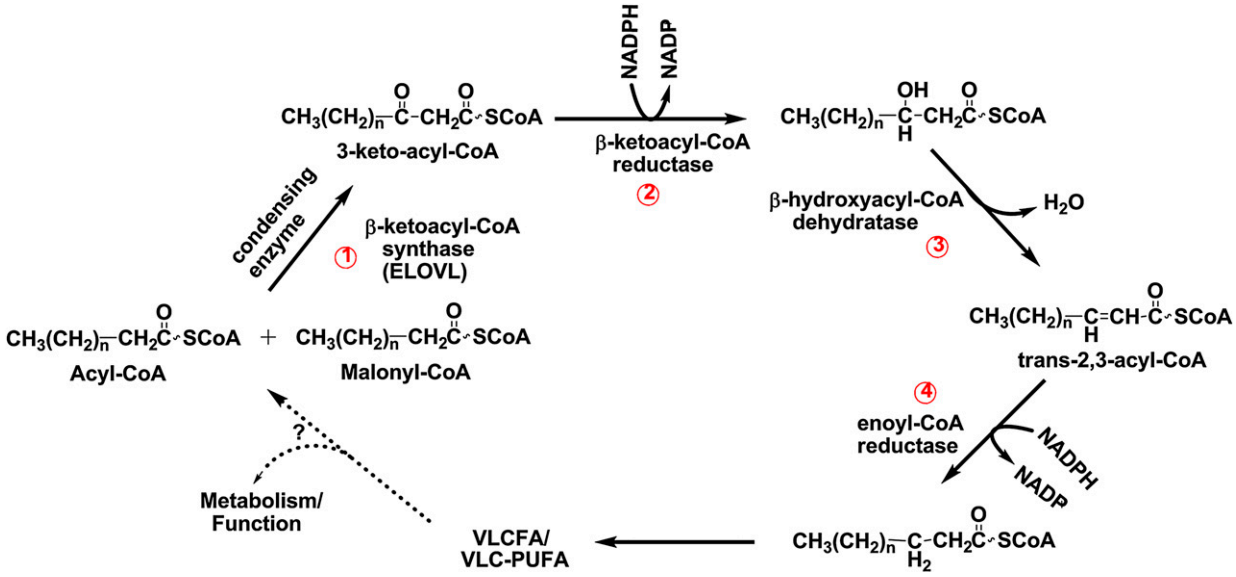

Fig. 2. The FA elongation system. The pathway of malonyl-CoA mediated elongation of fatty acyl-CoAs involves four enzymes and fatty acyl-CoA intermediates. Each round of elongation consists of four successive steps. Step 1 involves condensation of malonyl-CoA with the acyl-CoA substrate and is catalyzed by the elongase enzyme (ELOVL). Enzymes in this initial condensation step determine chain length and degree of unsaturation of the substrate; hence, this is the rate-limiting step of the elongation system. The product of the condensation reaction, the 3-keto-acyl-CoA, then undergoes a reduction catalyzed by a β-ketoacyl-CoA reductase (step 2) to produce 3-hydroxyacyl-CoA. Dehydration of the 3-hydroxyacyl-CoA by β-hydroxyacyl-CoA dehydratase (step 3) results in formation of *trans*-2,3-acyl-CoA, which is then reduced by enoyl-CoA reductase (step 4). Depending on the need of the specific cell or the organism at any particular time, the product is either utilized or undergoes additional round(s) of elongation.

gase gene identified (132) and was originally called cold-inducible glycoprotein of 30 kDa (*Cig30*) but was later renamed *Elovl3* (125, 132, 133). The *Elovl3* gene was proposed to encode an enzyme involved in biosynthesis of LC-FA in brown adipose tissue of mice exposed to cold stress. The ELOVL3 protein was proposed to be responsible for elongation of C24–C26 saturated FA and PUFA (125, 134, 135), based on studies from *Elovl3*$^{-/-}$ mice. Mouse *Elovl1* and *Elovl2* were identified later based on sequence homology to *Cig30* and were initially named *Ssc1* and *Ssc 2* (sequence similarity to *Cig 30*), respectively (104, 133). The ubiquitously expressed and proposed "housekeeping elongase" mouse ELOVL1 protein is involved in elongation of a broad range of saturated and monounsaturated FAs up to C26, which is used in sphingolipid formation (40, 122, 136). The protein has high expression levels between postnatal days 15 and 20 when 22:0 elongation is at its peak and synthesis of sphingolipids and myelin formation is taking place (40, 137). Thus, the function of the mouse ELOVL1 protein is similar to the yeast ELO3 protein (37, 104, 136). Vasireddy et al. (31) did not find significant message levels of *Elovl3* in the retina. This suggests that ELOVL1 and ELOVL3 may act on the same substrates in VLC-FA and VLC-PUFA biosynthesis.

ELOVL5 (HELO1) was the first human ELOVL protein to be identified (138) and, like mouse ELOVL2, elongates C18 to C20 and C20 to C22 (104, 124, 139) as well as monounsaturated 18:1, 20:1, and 22:1 (136). Both mouse and human ELOVL2 also elongates C22 to C24 PUFA of the n3 and n6 families, whereas the human ELOVL5 does not seem to be involved in elongations beyond C22 (104, 124, 136, 138).

The *ELOVL4* gene was discovered as a mutation associated with the cause of autosomal dominant STGD3 (118, 140–143). On the basis of its expression patterns, it was proposed to be involved in elongation of PUFA (118, 141). Using a gain-of-function approach, we found that the mouse ELOVL4 protein is involved in the elongation of C26–C28 saturated FA and PUFA and in the elongation of C28–C38 FA (39).

Inagakit et al. (144) identified two FA elongases in rats: rELO1 and rELO2. The human ELOVL5 and rELO1 are homologous and elongate C18 to C20 monounsaturated FA and PUFA (104, 136, 145, 146). When the *Elovl5* gene was deleted in mice, the C18 substrates of ELOVL5 protein accumulated with a resultant decrease in 22:6n3 and 20:4n6. (146). As a result, the *Elovl5* $^{-/-}$ mice developed fatty livers due to activation of sterol-regulatory element binding protein-1c and its target genes, which are negatively regulated by 22:6n3 and 20:4n6 (146). The mouse ELOVL6 protein elongates saturated FA from C12–C16 to C18 (104). When the human ELOVL6 protein was expressed in yeast cells, 16:0 levels decreased and 18:0, 18:1, and 20:0 levels increased (136). Also, levels of C20 and C22 FA were increased in yeast cells expressing human ELOVL6 (136). With the exception of *Elovl7*, *Elovl 1-6* messages have been shown to be present in different combinations in the mouse liver, skin, retina, and brain (31). Human ELOVL7 is the most recent member of the elongase family of proteins reported (147). It is expressed at high levels in adrenal glands, kidney, pancreas, and the prostate gland; lower

levels of expression occur in brain, placenta, and bone marrow (147). ELOVL7 has been reported to be upregulated in prostate cancer cells and tissues, and the ELOVL7 protein produced saturated C20–C24 FA that promoted prostate cancer growth in vivo in animals fed high-fat diets (147). Androgen was shown to stimulate the expression of ELOVL7, possibly through regulation by sterol-regulatory element binding protein-1 (147). Tumors in animals fed a high-fat diet were significantly increased in saturated C20–C24 FAs, testosterone, dihydrotestosterone, and *sphingosine 1-phosphate receptor 3* gene (147).

ELOVL1-7 transcripts are found in mouse, rat, bovine, porcine, monkey, and human. Mouse *Elovl1* is ubiquitously expressed, with the highest expression in the liver (31). Similarly, *Elovl2* is highly expressed in the mouse liver, testis, and retina (133, 148), but the retina has a relatively lower level of expression and the brain and skin have no detectable levels of the message (31). *Elovl3* expression occurs mainly in the liver, skin, and brown adipose tissues (133, 134), with no detectable mRNA expression found in the retina or brain (31, 149). *Elovl3* is also expressed in sebocytes of skin sebaceous glands and in the inner layer of the outer root sheath of hair follicles (104, 125). The liver has the highest expression of *Elovl5* and *Elovl6*, whereas *Elovl6* is expressed at low levels in the brain and retina and is not expressed in the skin (31). The tissue distribution of the *Elovl4* gene is discussed later in this review. Thus, differential expression of the *Elovl* genes exists in mammalian tissues, which reflects the different biosynthetic patterns of the variable chain lengths of FA found in these tissues. How the expression of each of these ELOVL enzymes is regulated is not yet completely understood.

STGD3 AND THE *ELOVL4* GENE

The recent interest in understanding the role of VLC-PUFA stems from the discovery that mutations in the *ELOVL4* gene are associated with STGD3, a rare form of Stargardt macular dystrophy (142, 143, 150–152). Clinically, it is very similar to the more common autosomal recessive Stargardt's disease (STGD1) to the extent that fundus (the inner interior surface of the eye) examination alone is not enough to distinguish between the two disorders (153). Donoso et al. (153) reported that STGD3 patients have a milder phenotype of the disease, have relatively good visual function, and minimal color vision defects without significant abnormalities in their electro-occulogram or electroretinogram (ERG) (154). Similar to STGD1, the onset of loss of vision in patients ranges from 3 to 50 years with a mean age of 14 years, while on the average, Snellen acuity of 20/200 occurred at an average age of 22 years. (155). Over decades, the macular lesion enlarges and visual acuity decreases to 20/300 to 20/800 (155). The typical phenotype usually seen in patients is a well-circumscribed homogenous atrophy of the retinal pigment epithelium, (RPE) and choriocapillaris in the macula surrounded by yellow flecks and temporal optic nerve pallor (155). **Figure 3** shows fundus photographs illustrating the typical phenotype and longitudinal follow-up of family members with the disease gene. Through the use of linkage analysis, the chromosomal loci were identified on 6q14 for STGD3 (151, 156–159). In 2001, two groups working independently used a positional candidate approach to identify a single 5-bp deletion (797-801 del AACTT) in exon 6 of the *ELOVL4* gene, which was associated with the disease in all affected members of STGD3/adMD families in independent North American kindreds (**Fig. 4A**) (118, 141). Also in 2001, Bernstein and his coworkers identified two mutations comprising 1-bp deletions separated by four nucleotides (790ΔT+794ΔT) within the same exon of the *ELOVL4* gene in a large, unrelated pedigree from Utah (Fig. 4B) (140). Another mutation (ELOVL4 p.Tyr270×) has also been identified in a European family with STGD3/adMD (162). It is interesting to note that these mutations occur within the same location in the exon 6 of the *ELOVL4* gene (142, 143). All of the mutations cause a frameshift that results in the introduction of a premature stop codon in the *ELOVL4* message, and hence premature termination of the protein with a resultant loss of the C-terminal endoplasmic reticulum retention/retrieval signal in the mutant protein. These strongly suggest that a loss of function of wild-type protein or mistargeting of the mutant protein underlies the pathology of the disease (118, 140). The exon 6 mutations in the *ELOVL4* gene and the subsequent truncation and loss of the last 45-51 amino acids at the carboxyl terminal end in the mutant protein (118, 141–143, 160) have been associated with STGD3 (140).

The ELOVL4 protein seems to be expressed only in those tissues that have VLC-PUFA (149). Thus the retina, which has the highest expression level of the ELOVL4 protein, has relatively higher VLC-PUFA levels of any organ so far examined. The highest protein expression was detected in the rod and cone photoreceptor inner segments and the outer nuclear layer of the retinas from different mammalian species (39, 149, 161–164). It is expressed to some extent in ganglion cell layers in human retinas (161, 163) and also in the brain (31, 149), testis (151), skin (31, 149), and lens (149). However, it is not expressed in the liver, kidney (141, 149), lung, or spleen (149).

The *ELOVL4* transcript was detected by Northern blot analysis, in situ hybridization, and qRT-PCR on embryonic days 11-17 in whole mouse embryos; expression peaked at day 15 and decreased by day 17 (143, 149, 161). Expression levels of the *Elovl4* mRNA in the brain and retina during postnatal development were also studied (149, 161). The highest level of expression was detected in the brain at postnatal day 1 (P1) and then declined gradually until P30, at which time it plateaued and remained constant throughout adult life (149). Significant expression of *Elovl4* was found in the eye at P1 (149, 161), doubled at P7 when photoreceptor outer segment development commenced, and increased gradually up to P30 (149, 161). A constant level of expression of *Elovl4* is found in the mouse retina from P45 to almost two years of age. In the adult retina, expression of the *Elovl4* mRNA and protein is mostly restricted to the outer nuclear layer and to the in-

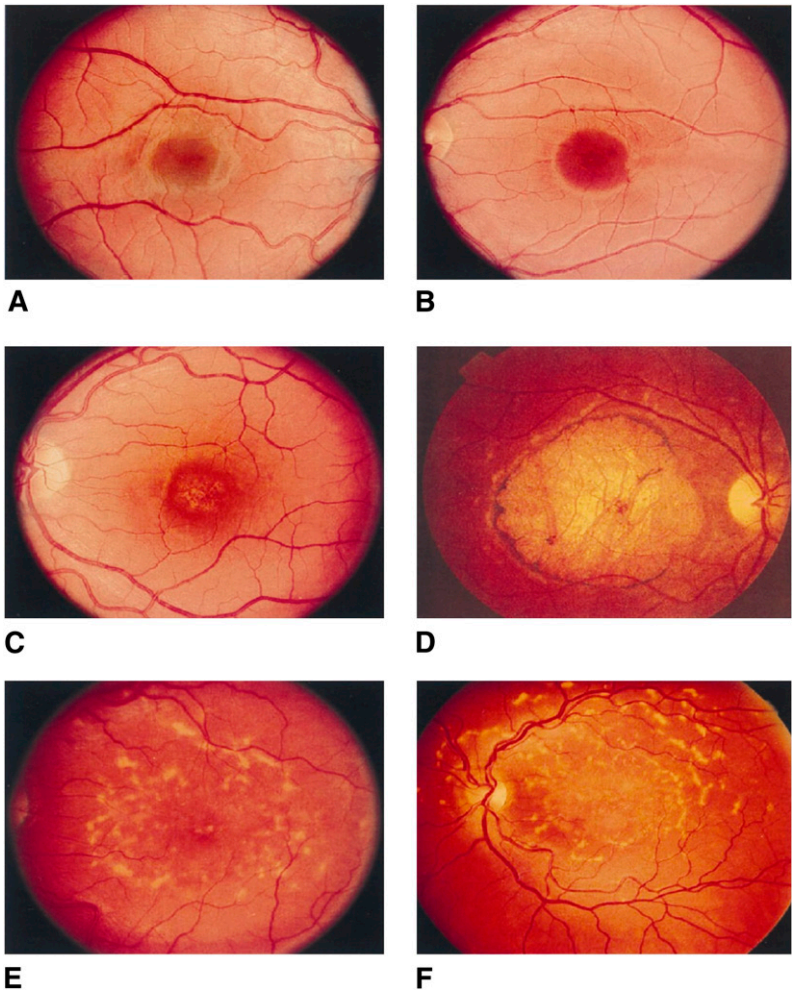

Fig. 3. Fundus photographs of STGD3 family members who inherited the disease gene that illustrate how the typical phenotype changes over time. A: Right eye of a 5 year-old boy (B VI-9) with the disease haplotype and normal fundus. B: Left eye of a 9 year-old boy (B VI-6) with visual acuity of 20/20, 1-year course of hemeralopia, and early foveal atrophy. C: Left eye of a 29 year-old man (B V-23) with a typical early lesion without flecks. D: Right eye of a 58 year-old man (A IV-25) with a typical late lesion with flecks. Longitudinal follow-up of the left eye of a woman (B III-15) at 45 (E) and 53 (F); note the increasing macular atrophy and fundus flecks (157). [Reprinted from Edwards et al. (157) with permission of Elsevier Science].

ner segments of both rod and cone photoreceptors (39, 161–163). Little expression of the message and protein is found in the inner retina. However, persistent expression occurs in postnatal whole lens without any dynamic changes (149).

ELOVL4 PROTEIN IS INVOLVED IN VLC-PUFA BIOSYNTHESIS

Until recently, the specific enzymes responsible for biosynthesis of VLC-PUFA remained elusive. To study the mechanism(s) of retinal degeneration in STGD3 patients, five independent transgenic mouse lines were developed. These include one transgenic, two knockout and two knockin lines (28, 30, 31, 143, 165–168). These mouse lines, to a large extent, contributed to our understanding of the function of the ELOVL4 protein as well as the disease mechanism of *Elovl4* mutations. The first evidence of the functional role of the ELOVL4 protein came from transgenic mice suggesting that the ELOVL4 protein could be involved in the elongation of FA chains > C26. When the *Elovl4* gene was deleted in mice (knockout), the homozygous pups died at birth (29, 166, 167). Similarly, animals that were homozygous for the mutations that cause macular degeneration in humans (knockin) also died perinatally (28, 30, 31). Close examination and investigation into the cause of the neonatal lethality in these mice revealed that they died of severe dehydration due to loss of skin permeability barrier (28–31). Analysis of the skin lipids revealed that they had significantly lower or absent levels of acyl-ceramides that contain long-chain saturated FAs beyond C26 (28–31). Also, McMahon et al. (32) found reduced retinal levels of PC-containing VLC-PUFA in their knockin *Elovl4* heterozygous mice (45). Using a direct gain-of-function approach, we showed that the mouse ELOVL4 protein is a component of an elongase system that elongates both saturated FAs and LC-PUFA from C26 to C28 and C28 to C30 FAs (39). When the ELOVL4 protein was expressed in rat neonatal cardiomyocytes and human ARPE-19 cells; supplementation with lignoceric acid (24:0), a precursor of VLC-FA (74, 169), led to its internalization and elongation to 28:0 and 30:0, indicating the involvement of ELOVL4 in the conversion of 26:0 to 28:0 and 28:0 to 30:0.

ELOVL4 IS A COMPONENT OF AN ELONGASE SYSTEM INVOLVED IN BIOSYNTHESIS OF VLC-PUFA

Studies in animal models indicated involvement of ELOVL4 in the biosynthesis of VLC-FA-containing ceramides in the skin (28–31). However, in the retina, sphin-

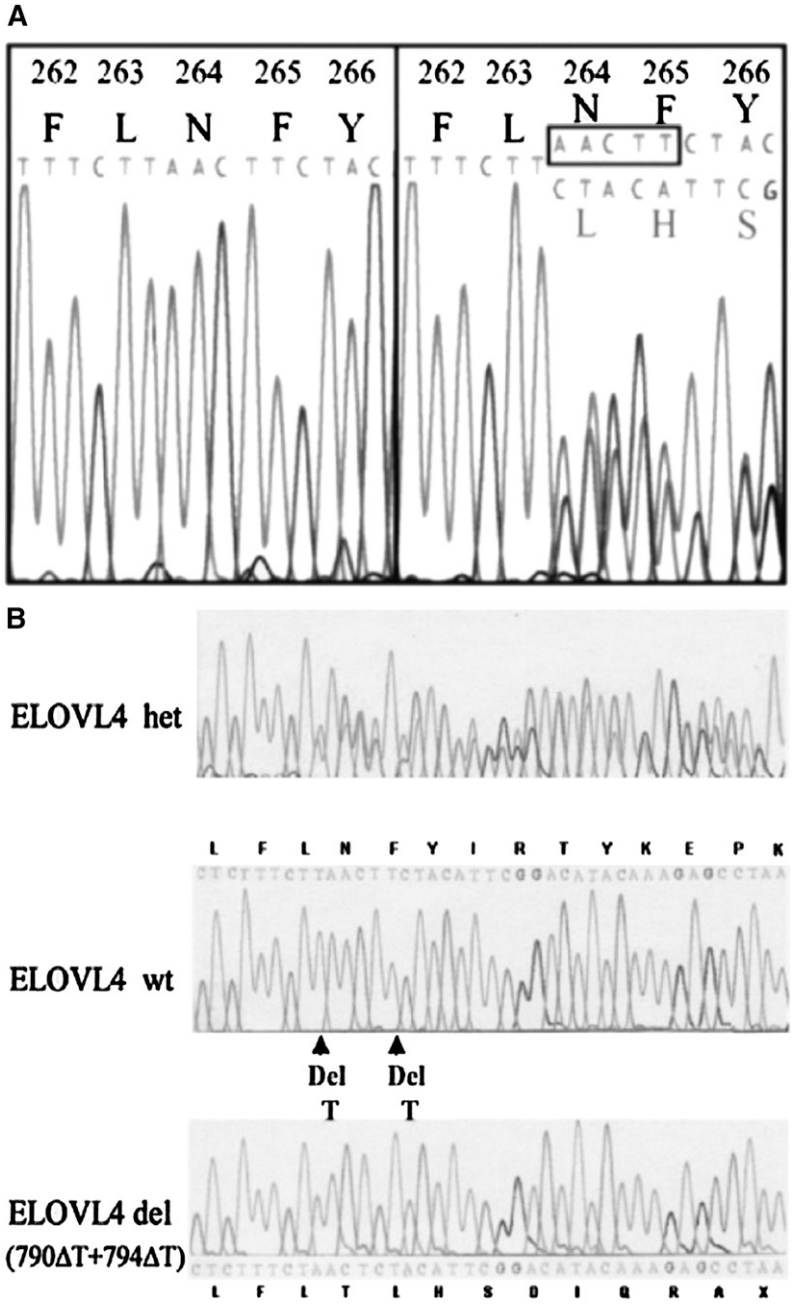

Fig. 4. Mutations in exon 6 of *ELOVL4* sequence from STGD3 patients. A: DNA sequence from exon 6 of *ELOVL4* from one unaffected (left) and one affected (right) family member. The affected family member is heterozygous. Clustering of the two DNA sequences demonstrate the deletion of the 5 bp segment AACTT in the affected patient (143). Reprinted from Edwards et al. (143) with permission from publishers. B: Complex deletions in the *ELOVL4* gene in patients from the K4175 pedigree. The panel shows a partial sequence of exon 6 from patient III-1 with the double deletion mutations (*ELOVL4* het). The nucleotide sequences and protein translations are shown above and below the direct-sequencing traces. The double deletion causes a frameshift that results in a premature stop codon after 10 amino acids (bottom trace). ELOVL4 wt, wild-type allele; ELOVL4 del (790ΔT+794ΔT), allele with the double deletion (142). Reprinted from Bernstein et al. (142) with permission from publishers.

golipids and ceramides are minor components of the lipid pool (33), whereas the retina contains higher amount of n3 and n6 VLC-PUFA esterified into PC molecular species (4). The retina also has the ability to synthesize VLC-PUFA from LC-PUFA precursors and acetate, although the elongase(s) responsible for their biosynthesis was not identified (5, 97, 98). We hypothesized that ELOVL4 protein is involved in the biosynthesis of the VLC-PUFA found in the retina, brain, and sperm since all of these tissues express ELOVL4 protein in higher quantities. We tested this hypothesis with *Elovl4*-transduced cardiomyocytes supplemented with eicosapentaenoic acid (20:5n3) and docosapentaenoic acid (22:5n3), which are precursors of VLC-PUFA. Nontransduced cells and cells transduced with Green Fluorescent Protein (*GFP*) or *Elovl4* gene elongated both precursors up to C24 and C26 n3 PUFA (independent of ELOVL4 expression) (**Fig. 5**). However, only *Elovl4*-transduced cells were able to further elongate each of these precursors to 28:5n3, 30:5n3, 32:5n3, 34:5n3, 36:5n3, and 38:5n3 (Fig. 5B, C). The major VLC-PUFA products in the *Elovl4*-transduced cells were 34:5n3 and 36:5n3 (39). We therefore proposed a pathway of VLC-PUFA biosynthesis in the retina and involvement of ELOVL4 protein in that scheme (**Fig. 6**). In addition, the products such as 34:6n3 and 36:6n3 could be the result of activity of desaturase enzymes (Fig. 6).

To determine whether VLC-PUFA formed from *Elovl4*-transduced cardiomyocytes treated with 20:5n3 were incorporated into ceramides, sphingomyelin, and PC, or remain as free FAs, we separated the total lipids into individual lipid classes by two-dimensional thin layer chromatography (39). The FA methyl esters from each class of

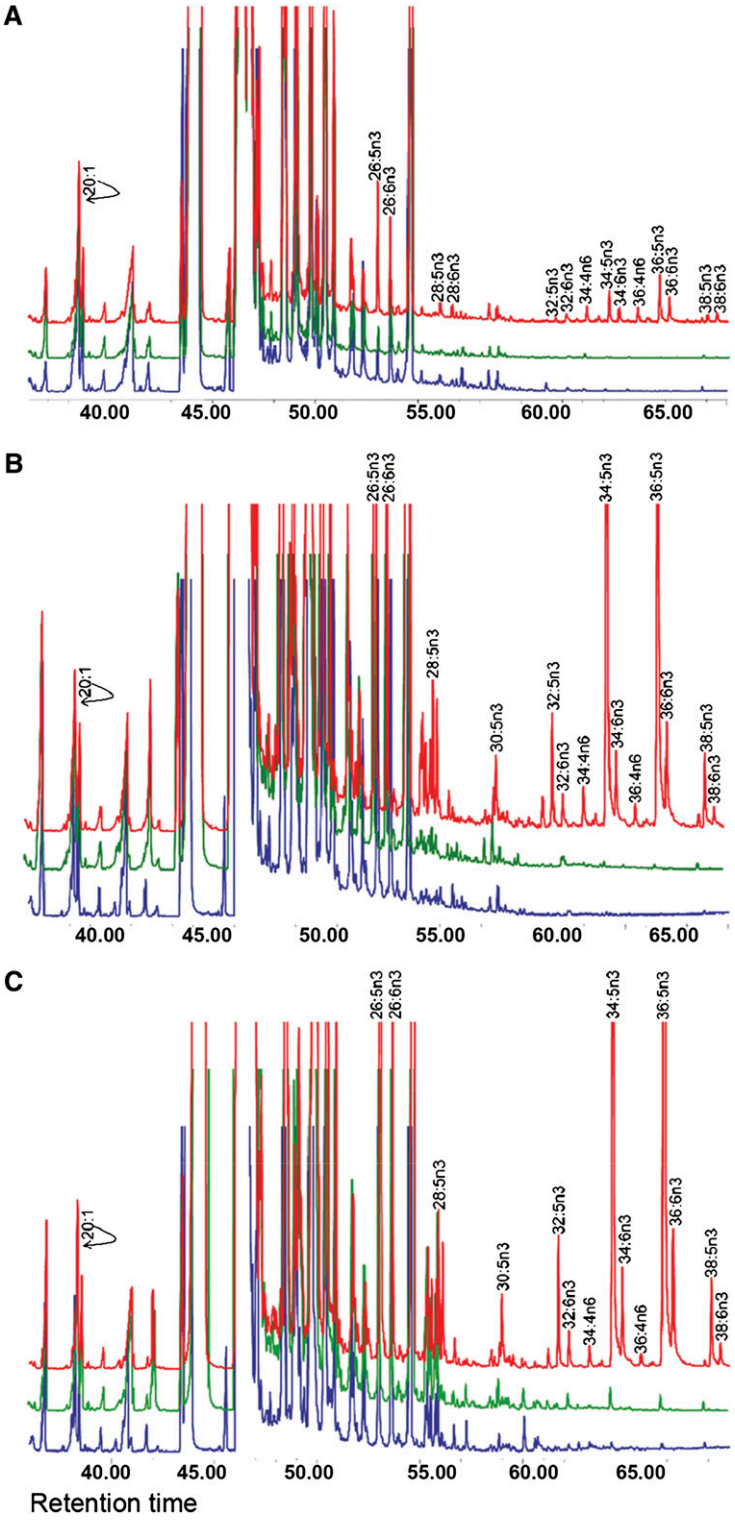

Fig. 5. Biosynthesis of VLC-PUFA in cardiomyocytes that express *Elovl4* transgene. GC-MS was used to identify the VLC-PUFA derived from cardiomyocytes treated with either 20:5n3 or 22:5n3 for 72 h after transduction with recombinant *Elovl4* or *GFP* viruses for 24 h. The PUFA response values were obtained by using the *m/z* ratios 79.1, 108.1, and 150.1 in SIM mode and abundances were compared by normalizing the chromatograms to the response of 20:1. A: Rat cardiomyocytes expressing mouse *Elovl4* (red) minigene or *GFP* (green) and nontransduced cells (blue) were cultured without precursors for 72 h. All cells, irrespective of ELOVL4 expression, synthesized C22-C26 PUFA. ELOVL4 expression in the absence of precursors resulted in the elongation of an endogenous precursor to C28-C38 VLC-PUFA. B: Cardiomyocytes in A above cultured with 20:5n3 synthesized C24-C26 in all treatment groups. Significant biosynthesis of C28–C38 n3 VLC-PUFA occurred in *Elovl4*-transduced cells (red), but not in *GFP* (green) and nontransduced cells (blue), with accumulation of 34:5n3 and 36:5n3. C: Cardiomyocytes in A above cultured with 22:5n3 synthesized C24-C26 in all treatment groups. They also synthesized the same n3 VLC-PUFA as found when 20:5n3 was used as the substrate. Note that each chromatogram was normalized to endogenous 20:1, which did not change among the sample groups. Reprinted from Agbaga et al. (39) with permission from publishers.

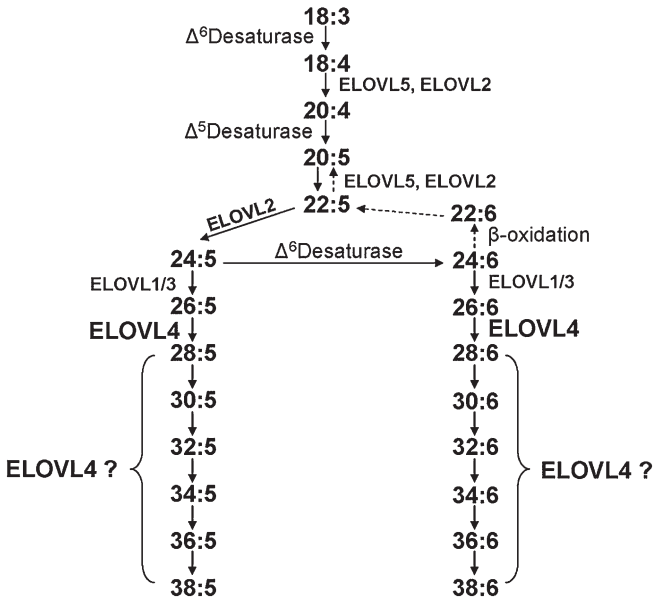

Fig. 6. Pathways of VLC-PUFA biosynthesis. Schematic diagram of in vivo n3 VLC-PUFA biosynthetic pathway mediated by ELOVL4 and other ELO families [modified after Suh and Clandinin (100)]. 18:3n3, 20:5n3, or 22:5n3 can be converted to VLC-PUFA through the consecutive enzymatic activities of desaturases and elongases. Although some elongases are specific for a single step, others are nonspecific or multifunctional and act at several steps (e.g., human ELOVL5 and murine ELOVL2) (126). We propose that ELOVL4 is essential for elongation of saturated 26:0 to 28:0 and of 26:5n3 to 28:5n3. It is also possible that ELOVL4 is necessary for generating (C30–C38):5n3, because these FAs are formed only in ELOVL4-expressing cells. However, other ELOVL proteins may be responsible for elongations of some of these VLC-PUFA (C30–C38) by using products generated by the ELOVL4 elongase activity. The synthesis of 34:6n3 and 36:6n3 in our study suggests desaturase activity on their shorter chain precursors. However, the specific desaturase(s) involved is not known. Reprinted from Agbaga et al. (39) with permission from publishers.

lipids were analyzed by GC-MS. We showed that the VLC-PUFA synthesized by ELOVL4 were present in PC, ceramides, sphingomyelin, and free FAs, but no VLC-PUFA were detectable in phosphatidylinositol, PE, or PS (39).

THE ROLE OF VLC-PUFA IN DISEASE

ELOVL4 is the elongase responsible for VLC FA biosynthesis and is present only in those tissues where the VLC-PUFA and VLC-FA are detected (28–31). The level of expression of ELOVL4 is highest in the retina and heterozygous mutations in the *ELOVL4* gene cause STGD3 in humans, but no other abnormalities in other ELOVL4 expressing tissues have been detected or reported in STGD3 patients. This could imply that VLC-PUFA and/or VLC-PUFA play a special role in the retina or that the quantity needed in retina is much higher than other tissues and the retinal cells with a heterozygous mutation in *ELOVL4* do not produce the required quantity of VLC-PUFAs. Indeed, in mouse models of heterozygous mutation in the *Elovl4* gene, reduction of VLC-PUFA content has been noted (32). Unfortunately, no homozygous mutation in human is known and therefore the pathological outcome of complete absence of ELOVL4 and therefore absence of VLC-PUFA in retina or any other tissues is not known.

Compared with *Elovl3* and *Elovl5* ablated mice that grew normally and were fertile (125, 135), the genetic mouse models with complete removal of functional ELOVL4 protein died at birth (28–31). This has so far been attributed to the abnormalities in the skin as they cannot form a proper permeability barrier due to lack of VLC-FA (mostly saturates) and die from dehydration (28–31). This establishes the role of VLC-FA in skin barrier permeability in that absence of these FAs results in neonatal lethality. The retinas of mice are not developed at the time they are born, so the effect of absence of VLC-PUFA in the retina has not been determined. Also, the retina contains higher levels of VLC-PUFA than VLC-FA and each may have different physiological roles. Very recently, McMahon et al., (2010) reported in an abstract the generation of transgenic mice expressing a wild-type *Elovl4* transgene under the control of an epidermis-specific *involucrin* promoter, which allowed skin-specific ELOVL4 expression. When bred into a homozygous *Elovl4* knockin background, the mice survived up to one month of age. This not only establishes the suggested hypothesis of neonatal death of ELOVL4 ablated mice, but also emphasizes its role in skin development (28–31, 170). The retinas of these mice were reported to have developed normally with properly organized multilayer structures of the retina. However, their ERG responses were half those of wild-type mice and the distal disks of the photoreceptor outer segments were disrupted with significant changes in RPE (171, 172). There was a complete absence of C28-C36-PC in a month-old retina. This suggests that VLC-PUFA may not be required for the development of the retina, but are important for its maintenance and function. However, the effect of the presence of two copies of the mutant ELOVL4 protein cannot be ignored in this model, since a dominant negative effect of mutant ELOVL4 protein has been shown in transgenic mouse lines (167) and in tissue culture studies. (152, 163, 173–175). It is still not clear if the retinal phenotype in mouse models of STGD3 is due to mislocalization of the mutant protein, generation of toxic products by the mutant protein, or the reduction in VLC-PUFA.

It is unlikely that VLC-PUFA redundantly serve the same purposes as the more common LC-PUFA such as docosahexaenoic acid (DHA) and arachidonic acid, which are already present in large amounts and are not reduced in the retina of heterozygote ELOVL4 knockout or knockin mice (28–31, 166, 167). We have shown that increasing DHA content of photoreceptor membranes of ELOVL4 transgenic mice (TG2 mice), which express one of the mutations identified in STGD3 (165) and recapitulate some aspects of the human disease, did not prevent retinal degeneration (176). To test the hypothesis that increasing DHA content of photoreceptor membranes of TG2 mice may prevent retinal degeneration, we bred TG2 mice to mice expressing the *Fat-1* transgene, which can convert n6

to n3 PUFA (123, 177, 178). After genotyping, Fat1^{+}/TG2^{+}, Fat1^{-}/TG2^{+}, Fat1^{+}/TG2^{-}, and Fat1^{-}/TG2^{-} mice were maintained on a diet deficient in n3 FAs but containing 10% safflower oil for 4 to 16 weeks. Although there were significantly higher levels of n3 PUFA (especially DHA) in liver, plasma, and retinas of mice expressing the fat-1 transgene compared with controls, there was no protection against retinal degeneration in the Fat1^{+}/TG2^{+} animals (176). By 16 weeks of age, despite having twice the amount of retinal DHA in *Fat-1* transgene-expressing mice compared with controls, the Fat1^{+}/TG2^{+} mice had reduced a-wave and b-wave ERG amplitudes, lower rhodopsin levels, and a significantly greater loss of photoreceptor cells compared with controls (176). These studies, coupled with the findings by McMahon et al. (32) showing reduced levels of VLC-PUFA in retinas of Elovl4 knockin mice that gradually accumulate A2E and lipofuscin in the retina (30), suggest that VLC-PUFA may be playing some uniquely important roles in the tissues where they are found and that these roles cannot be replaced by the more common LC-PUFAs. A therapeutic strategy of delivering VLC-PUFA to the retina could therefore have a promising outcome.

Besides their role in retinal physiology and diseases, VLC-PUFA may also have a role in neuroendocrine tumors, chronic pancreatitis, and adenocarcinoma metastases (179). By using methylation specific PCR, Omura et al, (2008) recently reported 68% methylation of *ELOVL4* in pancreatic cancers compared with 9% methylation in normal pancreas (180). Aberrant methylation that alters expression of a gene is the underlying cause of many human cancers and this important finding of methylation of the *ELOVL4* gene suggests possible involvement of VLC-FA or VLC-PUFA in cancer (180).

Under experimental induction of selective germ cell death in vivo, the VLC-PUFA disappeared from the testicular sphingomyelin and ceramides of adult fertile rats, suggesting that they associate with and play important roles in spermatogenic cells (19, 181–183). In more recent studies, delta-6-desaturase (D6D; or FA desaturase 2; FADS2) knockout mice (D6D$^{-/-}$) were unable to synthesize LC-PUFA and VLC-PUFA (184, 185). The D6D$^{-/-}$ mice lacked both n3 and n6 VLC-PUFAs and the males were sterile (184, 185). However, after dietary 22:6n3 (DHA) supplementation, the knockout males could synthesize 28:5n3, 28:6n3, and 30:6n3, and became fertile (185). Further studies showed that the supplemented DHA, possibly in combination with its elongated VLC-PUFA products, are required for flagellum and sperm head formation hence fertility.

THE ROLE OF VLC-PUFA IN MEMBRANE STRUCTURE AND FUNCTION

It is known that retinal outer segment membranes and other neural tissues contain high levels of n3 and n6 classes of LC-PUFA, which are essential membrane components and precursors of signaling molecules such as phosphatidylinositol, eicosanoids, and docosanoids (33, 186–189). These LC-PUFA-containing phospholipids mediate membrane fluidity, thereby modulating activities of ion channels and membrane-associated proteins or enzymes that require specific biophysical properties of lipid membranes for their normal function (190–192). For example, the whole phototransduction cascade from rhodopsin activation to opening and closing of nucleotide gated channels has been shown to be modulated by membrane LC-PUFA (43, 193–197). They also play important roles in the inflammatory response, growth, and development of neural tissues (198–200) and have exhibited anti-angiogenic, anti-vasoproliferative, and neuroproctective functions (34, 201, 202). Some classes of LC-PUFA are precursors of potent eicosanoids and docosanoids such as prostaglandins, leukotrienes, thromboxanes, neuroprotectins, and resolvins, which act as signaling molecules and serve other functions. Like LC-PUFA, the VLC-PUFA could also be the precursor of bioactive signaling molecules.

However, there are distinct structural differences between LC-PUFA and VLC-PUFA. Although retinal VLC-PUFA contain a similar number of double bonds with an n3 or n6 configuration, their carboxy-terminus has 12-20 additional carbons linked in single bonds. In a phospholipid structure, this would appear as a saturated stem followed by a bulky unsaturated tail (Fig. 1A–C). Such FAs may have a special function in forming membrane microdomains and in movement and activity of membrane proteins by forming pockets to bind cholesterol and proteins. It has been shown that sphingomyelin with FA lengths of C14–C24 interacted more strongly with cholesterol than a similar but monounsaturated series (203). If the VLC-PUFA span the bilayer, which they could due to their chain lengths, or even if they do not span the lipid bilayer of biological membrane as demonstrated in reconstituted pure lipid bilayers (43), the fluidity and packing density of each half of the bilayer would be quite different. This difference could be important for membranes that fold back on themselves, such as the rims of rod and cone outer segments. VLC-PUFA may have some role in forming those specialized structures in retinal photoreceptors and in the membranes of other cell types such as sperm and brain cells, which also contain VLC-PUFA. Similarly, cell structure and remodeling of membranes as pertains during retinal outer segment shedding may be dependent on coordinated interactions between lipid bilayers of the retinal outer segments and RPE. Thus the influence of plasma membrane lipids on biophysical properties of membrane curvature and elasticity cannot be underestimated (204, 205). Interestingly, *Elovl4* expression in the mouse retina accelerates at P7, which coincides with onset of rod outer segment morphogenesis (149). The PC-containing VLC-PUFA remain with the photo-inducible G-protein coupled receptor rhodopsin after repeated hexane extractions (206), implying that a tighter binding exists between VLC-PUFA and integral membrane proteins of rod outer segments. Aveldano et al. (206) proposed that the presence of VLC-PUFA at *sn-1* position in photoreceptor membrane PC may be responsible for binding rhodopsin in a way that makes the VLC-PUFA resistant to being separated from rhodopsin (206). They also hypothesized that the unusually long VLC-PUFA might partially surround the α-helical

segments of rhodopsin. Li et al. (207) recently demonstrated the existence of two acyl chains of an unknown phospholipid molecule bound tightly to the transmembrane loops H6 and H7 in the cytoplasmic half of rhodopsin crystal. From the studies of Brown et al. (208), Mitchell and Niu (43, 196, 197, 209) and others (210–215), we also know that membrane lipid bilayer has a direct influence on the energetics of the conformational states of rhodopsin in visual excitation. More recently Soubias et al. (213) used nuclear magnetic resonance and molecular dynamic simulations to provide evidence that there are specific sites on rhodopsin that bind the acyl chains of DHA. The binding was shown to be mainly in the grooves between the helixes of rhodopsin, thereby confirming previous studies (206, 207). Thus the findings that transgenic mice completely devoid of retinal C28-C36 acyl PC had impaired retinal function although the animals have normal retinal formation (172) suggest that VLC-PUFA together with LC-PUFA seem to play important roles in photoreceptor membrane function and possibly in other biological systems and that these roles cannot be replaced by the more common shorter chain FAs (C16-C18) or even the C20-C22 PUFA alone (214).

The FA composition of the membrane influences the transbilayer (flip-flop) motion of lipids (215) and may also be important in allowing the plasma membrane deformation for supple invagination during cleavage-furrow ingression (205) and in stabilizing membranes that are highly curved (216). This is especially important for retinal outer segments because their highly curved outer segments membranes recycle retinal that is released from rhodopsin apoprotein in the form of n-retinylidene–phosphatidylethanolamine (n-ret-PE). N-ret-PE transports retinal from the disk to the outer leaflet of photoreceptor membranes by a flip-flop mechanism with the aid of a large protein called ABCA4 (217, 218). Mutation in *ABCA4* gene is involved in the classical STGD1 (219–223) in humans. Interestingly, the pathology of STGD3 is very similar to STGD1. Like the *ABCA4* mutation-mediated pathology, the retinas of *Elovl4* transgenic (165) and knockin mice (30, 224) have been shown to have increased levels of lipofuscin and its precursor A2E (formed from condensation of PE and two molecules of all-*trans*-retinal) (225). We therefore speculate that VLC-PUFA produced by the ELOVL4 enzyme may be involved in the process of flip-flop activity of the membrane lipids and also in the activity of ABCA4 protein.

VLC-PUFA IN THE AGING RETINA

The amounts of VLC-PUFA containing lipids were found to be lower in the retina of older donor eyes (60-80 years) than in younger donor eyes (93). This decrease in VLC-PUFA content with age found in human donor eyes supports the earlier work of Rotstein et al. (56), which showed a decrease in VLC-PUFA content of phospholipids in the rat retina with increasing age. While 1.6 mol % VLC-PUFA were present in 2-3 month old rats, only 1.0% remained by age 26-27 months. This represents a 37% loss of VLC-PUFA in the retina of rats that are more than two years old (56). In addition to the decrease in VLC-PUFA in the retina with aging, a reduction in the degree of unsaturation also occurred. Rotstein et al. (56) also showed that the decrease in VLC-PUFA levels with aging was not due to an impaired activity of the enzymes involved in the synthesis and turnover of phospholipids, but was due to a decrease in the availability of these FAs in the retina. It is intriguing to speculate the functional relationship of this decrease in LC-PUFA and VLC-PUFA content in the human retina with a noted decline in the amplitude of ganzfeld-evoked ERG with age (226, 227). A study on 269 normal subjects by Birch et al. (226) showed an exponential decrease in rod and cone amplitudes, which declined by 50% by ages 69 to 70 years compared with the young adults aged 15–24 years. Naash et al. (228) showed that rod- and cone-mediated ERG amplitudes were lower in older mice than in younger mice. Considering our knowledge of the role of LC-PUFA in phototransduction (196, 197, 229–235), it is possible that apart from other age-related changes that may affect retina function, there may be an association between the decline in VLC-PUFA content with age and the decrease in ERG amplitudes.

CONCLUSION

At this point, we know very little about the function of VLC-PUFA in tissues and cells in which they are found. However, studies on the role of LC-PUFA in retina over the years have provided some insights for us to better define as well as speculate on the function of VLC-PUFA in the retina. We think that VLC-PUFA, similar to LC-PUFA in the retina, have the capability of modulating four broad targets, none of which are independent of the other (236, 237). These targets include photoreceptor membrane organization (238) and function, cellular signaling (194–196, 209), gene expression, and possibly generation of a potent class of novel molecules that can act in an autocrine or paracrine function in maintaining the structure and function of the retina (201, 202, 239, 240).

It is likely that reduction or lack of VLC-PUFA products in the retinas of STGD3 patients contributes to STGD3 pathology. However, we do not rule out the possibility of toxic effects exerted by the mutant protein or its products in contributing to the retinal phenotype. Because ELOVL4 is involved in an important retinal disease and is currently the only known enzyme involved in biosynthesis of VLC-PUFA, the need exists to take a closer look at the roles of these FA in disease and health, exploring and elucidating the functional and physiological roles of VLC-PUFA in the tissues where they are found.

We apologize for not being able to cite all publications relevant to LC-PUFA and VLC-PUFA function in the various tissues. We thank Steve Brush for his comments and suggestions in preparation of this work.

REFERENCES

1. Rezanka, T. 1989. Very-long-chain fatty acids from the animal and plant kingdoms. *Prog. Lipid Res.* **28:** 147–187.
2. Tvrzicka, E., T. Rezanka, J. Krijt, and V. Janousek. 1988. Identification of very-long- chain fatty acids in rat and mouse harderian gland lipids by capillary gas chromatography-mass spectrometry. *J. Chromatogr.* **431:** 231–238.
3. Poulos, A. 1995. Very long chain fatty acids in higher animals–a review. *Lipids.* **30:** 1–14.
4. Aveldano, M. I. 1987. A novel group of very long chain polyenoic fatty acids in dipolyunsaturated phosphatidylcholines from vertebrate retina. *J. Biol. Chem.* **262:** 1172–1179.
5. Rotstein, N. P., and M. I. Aveldano. 1988. Synthesis of very long chain (up to 36 carbon) tetra, penta and hexaenoic fatty acids in retina. *Biochem. J.* **249:** 191–200.
6. Aveldano, M. I., and H. Sprecher. 1987. Very long chain (C24 to C36) polyenoic fatty acids of the n-3 and n-6 series in dipolyunsaturated phosphatidylcholines from bovine retina. *J. Biol. Chem.* **262:** 1180–1186.
7. Tiffany, J. M. 1987. The lipid secretion of the meibomian glands. *Adv. Lipid Res.* **22:** 1–62.
8. Harvey, D. J., J. M. Tiffany, J. M. Duerden, K. S. Pandher, and L. S. Mengher. 1987. Identification by combined gas chromatography-mass spectrometry of constituent long- chain fatty acids and alcohols from the meibomian glands of the rat and a comparison with human meibomian lipids. *J. Chromatogr.* **414:** 253–263.
9. Rezanka, T., and K. Sigler. 2009. Odd-numbered very-long-chain fatty acids from the microbial, animal and plant kingdoms. *Prog. Lipid Res.* **48:** 206–238.
10. Rezanka, T., and V. M. Dembitsky. 2004. Tetratriacontanonaenoic acid, first natural acid with nine double bonds isolated from a crustacean Bathynella natans. *Tetrahedron.* **60:** 4261–4264.
11. Rezanka, T., L. Nedbalova, and K. Sigler. 2008. Odd-numbered very-long-chain polyunsaturated fatty acids from the dinoflagellate Amphidinium carterae identified by atmospheric pressure chemical ionization liquid chromatography-mass spectrometry. *Phytochemistry.* **69:** 2849–2855.
12. Rezanka, T., L. Nedbalova, and K. Sigler. 2008. Identification of very-long-chain polyunsaturated fatty acids from Amphidinium carterae by atmospheric pressure chemical ionization liquid chromatography-mass spectroscopy. *Phytochemistry.* **69:** 2391–2399.
13. Rezanka, T., L. Nedbalova, K. Sigler, and V. Cepak. 2008. Identification of astaxanthin diglucoside diesters from snow alga Chlamydomonas nivalis by liquid chromatography-atmospheric pressure chemical ionization mass spectrometry. *Phytochemistry.* **69:** 479–490.
14. Rodkina, S. A. 2005. Fatty acids and other lipids of marine sponges. *Russ. J. Mar. Biol.* **31:** S49–S60.
15. Mishra, P. M., and A. Sree. 2008. Composition of the lipophilic extract from the sponge *Axinella carteri* collected from the Bay of Bengal of the Orissa coast. *Chem. Nat. Compd.* **44:** 282–286.
16. Poulos, A., P. Sharp, D. Johnson, and C. Easton. 1988. The occurrence of polyenoic very long chain fatty acids with greater than 32 carbon atoms in molecular species of phosphatidylcholine in normal and peroxisome-deficient (Zellweger's syndrome) brain. *Biochem. J.* **253:** 645–650.
17. Aveldano, M. I., B. S. Robinson, D. W. Johnson, and A. Poulos. 1993. Long and very long chain polyunsaturated fatty acids of the n-6 series in rat seminiferous tubules. Active desaturation of 24:4n-6 to 24:5n-6 and concomitant formation of odd and even chain tetraenoic and pentaenoic fatty acids up to C32. *J. Biol. Chem.* **268:** 11663–11669.
18. Furland, N. E., G. M. Oresti, S. S. Antollini, A. Venturino, E. N. Maldonado, and M. I. Aveldano. 2007. Very long-chain polyunsaturated fatty acids are the major acyl groups of sphingomyelins and ceramides in the head of mammalian spermatozoa. *J. Biol. Chem.* **282:** 18151–18161.
19. Furland, N. E., S. R. Zanetti, G. M. Oresti, E. N. Maldonado, and M. I. Aveldano. 2007. Ceramides and sphingomyelins with high proportions of very long-chain polyunsaturated fatty acids in mammalian germ cells. *J. Biol. Chem.* **282:** 18141–18150.
20. Poulos, A., P. Sharp, H. Singh, D. Johnson, A. Fellenberg, and A. Pollard. 1986. Detection of a homologous series of C26–C38 polyenoic fatty acids in the brain of patients without peroxisomes (Zellweger's syndrome). *Biochem. J.* **235:** 607–610.
21. Poulos, A., K. Beckman, D. W. Johnson, B. C. Paton, B. S. Robinson, P. Sharp, S. Usher, and H. Singh. 1992. Very long-chain fatty acids in peroxisomal disease. *Adv. Exp. Med. Biol.* **318:** 331–340.
22. Butovich, I. A. 2009. Cholesteryl esters as a depot for very long chain fatty acids in human meibum. *J. Lipid Res.* **50:** 501–513.
23. Butovich, I. A., J. Wojtowicz, and M. Molai. 2009. Human tear film and meibum. I. Very long chain wax esters and (O-acyl)-omega-hydroxy fatty acids of meibum. *J. Lipid Res.* **50:** 2471–2785.
24. Butovich, I. A. 2008. On the lipid composition of human meibum and tears: comparative analysis of nonpolar lipids. *Invest. Ophthalmol. Vis. Sci.* **49:** 3779–3789.
25. Butovich, I. A., E. Uchiyama, and J. P. McCulley. 2007. Lipids of human meibum: mass-spectrometric analysis and structural elucidation. *J. Lipid Res.* **48:** 2220–2235.
26. Butovich, I. A. 2009. The Meibomian puzzle: combining pieces together. *Prog. Retin. Eye Res.* **28:** 483–498.
27. Butovich, I. A., J. C. Wojtowicz, and M. Molai. 2009. Human tear film and meibum. Very long chain wax esters and (O-acyl)-omega-hydroxy fatty acids of meibum. *J. Lipid Res.* **50:** 2471–2485.
28. Cameron, D. J., Z. Tong, Z. Yang, J. Kaminoh, S. Kamiyah, H. Chen, J. Zeng, Y. Chen, L. Luo, and K. Zhang. 2007. Essential role of Elovl4 in very long chain fatty acid synthesis, skin permeability barrier function, and neonatal survival. *Int. J. Biol. Sci.* **3:** 111–119.
29. Li, W., R. Sandhoff, M. Kono, P. Zerfas, V. Hoffmann, B. C. Ding, R. L. Proia, and C. X. Deng. 2007. Depletion of ceramides with very long chain fatty acids causes defective skin permeability barrier function, and neonatal lethality in ELOVL4 deficient mice. *Int. J. Biol. Sci.* **3:** 120–128.
30. McMahon, A., I. A. Butovich, N. L. Mata, M. Klein, R. Ritter 3rd, J. Richardson, D. G. Birch, A. O. Edwards, and W. Kedzierski. 2007. Retinal pathology and skin barrier defect in mice carrying a Stargardt disease-3 mutation in elongase of very long chain fatty acids-4. *Mol. Vis.* **13:** 258–272.
31. Vasireddy, V., Y. Uchida, N. Salem, Jr., S. Y. Kim, M. N. Mandal, G. B. Reddy, R. Bodepudi, N. L. Alderson, J. C. Brown, H. Hama, et al. 2007. Loss of functional ELOVL4 depletes very long-chain fatty acids (> or =C28) and the unique omega-O-acylceramides in skin leading to neonatal death. *Hum. Mol. Genet.* **16:** 471–482.
32. McMahon, A., S. N. Jackson, A. S. Woods, and W. Kedzierski. 2007. A Stargardt disease-3 mutation in the mouse Elovl4 gene causes retinal deficiency of C32–C36 acyl phosphatidylcholines. *FEBS Lett.* **581:** 5459–5463.
33. Fliesler, S. J., and R. E. Anderson. 1983. Chemistry and metabolism of lipids in the vertebrate retina. *Prog. Lipid Res.* **22:** 79–131.
34. SanGiovanni, J. P., and E. Y. Chew. 2005. The role of omega-3 long-chain polyunsaturated fatty acids in health and disease of the retina. *Prog. Retin. Eye Res.* **24:** 87–138.
35. Neuringer, M., and B. G. Jeffrey. 2003. Visual development: neural basis and new assessment methods. *J. Pediatr.* **143:** S87–S95.
36. Bazan, N. G. 2007. Homeostatic regulation of photoreceptor cell integrity: significance of the potent mediator neuroprotectin D1 biosynthesized from docosahexaenoic acid: the Proctor Lecture. *Invest Ophthalmol Vis Sci* **48**: 4866–4881; biography 4864–4865.
37. Oh, C. S., D. A. Toke, S. Mandala, and C. E. Martin. 1997. ELO2 and ELO3, homologues of the Saccharomyces cerevisiae ELO1 gene, function in fatty acid elongation and are required for sphingolipid formation. *J. Biol. Chem.* **272:** 17376–17384.
38. Schneiter, R., V. Tatzer, G. Gogg, E. Leitner, and S. D. Kohlwein. 2000. Elo1p- dependent carboxy-terminal elongation of C14: 1Delta(9) to C16:1Delta(11) fatty acids in Saccharomyces cerevisiae. *J. Bacteriol.* **182:** 3655–3660.
39. Agbaga, M. P., R. S. Brush, M. N. Mandal, K. Henry, M. H. Elliott, and R. E. Anderson. 2008. Role of Stargardt-3 macular dystrophy protein (ELOVL4) in the biosynthesis of very long chain fatty acids. *Proc. Natl. Acad. Sci. USA.* **105:** 12843–12848.
40. Guillou, H., D. Zadravec, P. G. Martin, and A. Jacobsson. 2010. The key roles of elongases and desaturases in mammalian fatty acid metabolism: Insights from transgenic mice. *Prog. Lipid Res.* **49:** 186–199.
41. Kawamura, N., A. B. Moser, H. W. Moser, T. Ogino, K. Suzuki, H. Schaumburg, A. Milunsky, J. Murphy, and Y. Kishimoto. 1978. High concentration of hexacosanoate in cultured skin fibroblast lipids from adrenoleukodystrophy patients. *Biochem. Biophys. Res. Commun.* **82:** 114–120.
42. Rezanka, T., and J. Votruba. 2005. Analysis of fatty acids by APCI-MS. *In* Modern Methods for Lipid Analysis by LC-MS

and Related Techniques. Byrdwell WC, editor. AOSC Press, Champaign, IL. 242–275.
43. Mitchell, D. C., S-L. Niu, M. Bennett, L. A. Greeley, K. G. Hines, and B. M. Andersen. 2007. Effects of ROS disk membrane phospholipids with extremely long polyunsaturated acyl chains on visual signalling. *Invest. Ophthalmol. Vis. Sci.* **48:** 2928.
44. Infante, J. P., C. L. Tschanz, N. Shaw, A. L. Michaud, P. Lawrence, and J. T. Brenna. 2002. Straight-chain acyl-CoA oxidase knockout mouse accumulates extremely long chain fatty acids from alpha-linolenic acid: evidence for runaway carousel-type enzyme kinetics in peroxisomal beta-oxidation diseases. *Mol. Genet. Metab.* **75:** 108–119.
45. McMahon, A., and W. Kedzierski. Polyunsaturated extremely long chain C28–C36 fatty acids and retinal physiology. *Br. J. Ophthalmol.* Epub ahead of print. August 9, 2009.
46. Carpenter, M. P. 1971. The lipid composition of maturing rat testis. The effect of alpha- tocopherol. *Biochim. Biophys. Acta.* **231:** 52–79.
47. Holman, R. T., and H. H. Hofstetter. 1965. The fatty acid composition of the lipids from bovine and porcine reproductive tissues. *J. Am. Oil Chem. Soc.* **42:** 540–544.
48 Davis, J. T., R. B. Bridges, and J. G. Coniglio. 1966. Changes in lipid composition of the maturing rat testis. *Biochem. J.* **98:** 342–346.
49. Bridges, R. B., and J. G. Coniglio. 1970. The metabolism of 4,7,10,13,16-(5–14C)docosapentaenoic acid in the testis of the rat. *Biochim. Biophys. Acta.* **218:** 29–35.
50. Bridges, R. B., and J. G. Coniglio. 1970. The biosynthesis of delta-9,12,15,18- tetracosatetraenoic and of delta-6,9,12,15,18-tetracosapentaenoic acids by rat testes. *J. Biol. Chem.* **245:** 46–49.
51. Grogan, W. M., and J. W. Lam. 1982. Fatty acid synthesis in isolated spermatocytes and spermatids of mouse testis. *Lipids.* **17:** 604–611.
52. Grogan, W. M., and E. G. Huth. 1983. Biosynthesis of long-chain polyenoic acids from arachidonic acid in cultures of enriched spermatocytes and spermatids from mouse testis. *Lipids.* **18:** 275–284.
53. Grogan, W. M. 1984. Metabolism of arachidonate in rat testis: characterization of 26–30 carbon polyenoic acids. *Lipids.* **19:** 341–346.
54. Poulos, A., P. Sharp, D. Johnson, I. White, and A. Fellenberg. 1986. The occurrence of polyenoic fatty acids with greater than 22 carbon atoms in mammalian spermatozoa. *Biochem. J.* **240:** 891–895.
55. Poulos, A., D. W. Johnson, K. Beckman, I. G. White, and C. Easton. 1987. Occurrence of unusual molecular species of sphingomyelin containing 28–34-carbon polyenoic fatty acids in ram spermatozoa. *Biochem. J.* **248:** 961–964.
56. Rotstein, N. P., M. G. Ilincheta de Boschero, N. M. Giusto, and M. I. Aveldano. 1987. Effects of aging on the composition and metabolism of docosahexaenoate-containing lipids of retina. *Lipids.* **22:** 253–260.
57. Robinson, B. S., D. W. Johnson, and A. Poulos. 1992. Novel molecular species of sphingomyelin containing 2-hydroxylated polyenoic very-long-chain fatty acids in mammalian testes and spermatozoa. *J. Biol. Chem.* **267:** 1746–1751.
58. Robinson, B. S., D. W. Johnson, and A. Poulos. 1990. Metabolism of hexacosatetraenoic acid (C26:4,n-6) in immature rat brain. *Biochem. J.* **267:** 561–564.
59. Sharp, P., A. Poulos, A. Fellenberg, and D. Johnson. 1987. Structure and lipid distribution of polyenoic very-long-chain fatty acids in the brain of peroxisome- deficient patients (Zellweger syndrome). *Biochem. J.* **248:** 61–67.
60. Pullarkat, R. K., and H. Reha. 1976. Distribution of positional isomers of monoenoic fatty acids in pig-brain white matter sphingolipids. *J. Neurochem.* **27:** 321–322.
61. Johnson, D. W., K. Beckman, A. J. Fellenberg, B. S. Robinson, and A. Poulos. 1992. Monoenoic fatty acids in human brain lipids: isomer identification and distribution. *Lipids.* **27:** 177–180.
62. Robinson, B. S., D. W. Johnson, and A. Poulos. 1990. Unique molecular species of phosphatidylcholine containing very-long-chain (C24–C38) polyenoic fatty acids in rat brain. *Biochem. J.* **265:** 763–767.
63. Sharp, P., D. Johnson, and A. Poulos. 1991. Molecular species of phosphatidylcholine containing very long chain fatty acids in human brain: enrichment in X-linked adrenoleukodystrophy brain and diseases of peroxisome biogenesis brain. *J. Neurochem.* **56:** 30–37.
64. Aveldano, M. I., M. VanRollins, and L. A. Horrocks. 1983. Separation and quantitation of free fatty acids and fatty acid methyl esters by reverse phase high pressure liquid chromatography. *J. Lipid Res.* **24:** 83–93.
65. Abe, K., and Y. Tamai. 1982. Simultaneous determination of methyl esters of alpha- hydroxy and nonhydroxy fatty acids from brain cerebroside by fused-silica capillary gas chromatography. *J. Chromatogr.* **232:** 400–405.
66. Odutuga, A. A., E. M. Carey, and R. E. Prout. 1973. Changes in the lipid and fatty acid composition of developing rabbit brain. *Biochim. Biophys. Acta.* **316:** 115–123.
67. Poulos, A. 1989. Lipid metabolism in Zellweger's syndrome. *Prog. Lipid Res.* **28:** 35–51.
68. Moser, A. E., I. Singh, F. R. Brown 3rd, G. I. Solish, R. I. Kelley, P. J. Benke, and H. W. Moser. 1984. The cerebrohepatorenal (Zellweger) syndrome. Increased levels and impaired degradation of very-long-chain fatty acids and their use in prenatal diagnosis. *N. Engl. J. Med.* **310:** 1141–1146.
69. Igarashi, M., H. H. Schaumburg, J. Powers, Y. Kishmoto, E. Kolodny, and K. Suzuki. 1976. Fatty acid abnormality in adrenoleukodystrophy. *J. Neurochem.* **26:** 851–860.
70. Aveldano, M. I., and D. Donnari. 1996. Plasma phospholipid fatty acids in X-linked adrenoleukodystrophy. *Clin. Chem.* **42:** 454–461.
71. Poulos, A., P. Sharp, A. J. Fellenberg, and D. W. Johnson. 1988. Accumulation of pristanic acid (2, 6, 10, 14 tetramethylpentadecanoic acid) in the plasma of patients with generalised peroxisomal dysfunction. *Eur. J. Pediatr.* **147:** 143–147.
72. Singh, I., A. E. Moser, S. Goldfischer, and H. W. Moser. 1984. Lignoceric acid is oxidized in the peroxisome: implications for the Zellweger cerebro-hepato-renal syndrome and adrenoleukodystrophy. *Proc. Natl. Acad. Sci. USA.* **81:** 4203–4207.
73. Singh, I., A. E. Moser, H. W. Moser, and Y. Kishimoto. 1984. Adrenoleukodystrophy: impaired oxidation of very long chain fatty acids in white blood cells, cultured skin fibroblasts, and amniocytes. *Pediatr. Res.* **18:** 286–290.
74. Street, J. M., H. Singh, and A. Poulos. 1990. Metabolism of saturated and polyunsaturated very-long-chain fatty acids in fibroblasts from patients with defects in peroxisomal beta-oxidation. *Biochem. J.* **269:** 671–677.
75. Brites, P., P. A. Mooyer, L. El Mrabet, H. R. Waterham, and R. J. Wanders. 2009. Plasmalogens participate in very-long-chain fatty acid-induced pathology. *Brain.* **132:** 482–492.
76. Singh, J., M. Khan, and I. Singh. 2009. Silencing of Abcd1 and Abcd2 genes sensitizes astrocytes for inflammation: implication for X-adrenoleukodystrophy. *J. Lipid Res.* **50:** 135–147.
77. Chung, T. C., H. S. Kou, M. C. Chao, Y. J. Ou, and H. L. Wu. 2008. A simple and sensitive liquid chromatographic method for the analysis of free docosanoic, tetracosanoic and hexacosanoic acids in human plasma as fluorescent derivatives. *Anal. Chim. Acta.* **611:** 113–118.
78. Fan, C. Y., J. Pan, R. Chu, D. Lee, K. D. Kluckman, N. Usuda, I. Singh, A. V. Yeldandi, M. S. Rao, N. Maeda, et al. 1996. Targeted disruption of the peroxisomal fatty acyl-CoA oxidase gene: generation of a mouse model of pseudoneonatal adrenoleukodystrophy. *Ann. N. Y. Acad. Sci.* **804:** 530–541.
79. Fan, C. Y., J. Pan, R. Chu, D. Lee, K. D. Kluckman, N. Usuda, I. Singh, A. V. Yeldandi, M. S. Rao, N. Maeda, et al. 1996. Hepatocellular and hepatic peroxisomal alterations in mice with a disrupted peroxisomal fatty acyl-coenzyme A oxidase gene. *J. Biol. Chem.* **271:** 24698–24710.
80. Christensen, E., B. Woldseth, T. A. Hagve, B. T. Poll-The, R. J. Wanders, H. Sprecher, O. Stokke, and B. O. Christophersen. 1993. Peroxisomal beta-oxidation of polyunsaturated long chain fatty acids in human fibroblasts. The polyunsaturated and the saturated long chain fatty acids are retroconverted by the same acyl-CoA oxidase. *Scand. J. Clin. Lab. Invest. Suppl.* **215:** 61–74.
81. Reddy, J. K., and T. Hashimoto. 2001. Peroxisomal beta-oxidation and peroxisome proliferator-activated receptor alpha: an adaptive metabolic system. *Annu. Rev. Nutr.* **21:** 193–230.
82. Asselineau, C., J. Asselineau, G. Laneelle, and M. A. Laneelle. 2002. The biosynthesis of mycolic acids by Mycobacteria: current and alternative hypotheses. *Prog. Lipid Res.* **41:** 501–523.
83. Tiffany, J. M. 1978. Individual variations in human meibomian lipid composition. *Exp. Eye Res.* **27:** 289–300.
84. Tiffany, J. M. 1979. The meibomian lipids of the rabbit. I. Overall composition. *Exp. Eye Res.* **29:** 195–202.

85. Nicolaides, N., J. K. Kaitaranta, T. N. Rawdah, J. I. Macy, F. M. Boswell 3rd, and R. E. Smith. 1981. Meibomian gland studies: comparison of steer and human lipids. *Invest. Ophthalmol. Vis. Sci.* **20:** 522–536.
86. Harvey, D. J., and J. M. Tiffany. 1984. Identification of meibomian gland lipids by gas chromatography-mass spectrometry: application to the meibomian lipids of the mouse. *J. Chromatogr.* **301:** 173–187.
87. Mathers, W. D., and J. A. Lane. 1998. Meibomian gland lipids, evaporation, and tear film stability. *Adv. Exp. Med. Biol.* **438:** 349–360.
88. Nicolaides, N., E. C. Santos, and K. Papadakis. 1984. Double-bond patterns of fatty acids and alcohols in steer and human meibomian gland lipids. *Lipids.* **19:** 264–277.
89. Nicolaides, N., E. C. Santos, K. Papadakis, E. C. Ruth, and L. Muller. 1984. The occurrence of long chain alpha, omega-diols in the lipids of steer and human meibomian glands. *Lipids.* **19:** 990–993.
90. Frankel, E. N. 1980. Lipid oxidation. *Prog. Lipid Res.* **19:** 1–22.
91. Frankel, E. N. 1984. Chemistry of free radical and singlet oxidation of lipids. *Prog. Lipid Res.* **23:** 197–221.
92. Frankel, E. N., T. Satue-Gracia, A. S. Meyer, and J. B. German. 2002. Oxidative stability of fish and algae oils containing long-chain polyunsaturated fatty acids in bulk and in oil-in-water emulsions. *J. Agric. Food Chem.* **50:** 2094–2099.
93. Liu, A., J. Chang, Z. Shen, and P. S. Bernstein. 2009. Enhanced methods for analysis of very long chain polyunsaturated fatty acids from retina and RPE. *Invest. Ophthalmol. Vis. Sci.* **50:** E-abstract 3410.
94. Rosenthal, M. D., M. C. Garcia, M. R. Jones, and H. Sprecher. 1991. Retroconversion and delta 4 desaturation of docosatetraenoate (22:4(n-6) and docosapentaenoate (22:5(n-3) by human cells in culture. *Biochim. Biophys. Acta.* **1083:** 29–36.
95. Garcia, M. C., H. Sprecher, and M. D. Rosenthal. 1990. Chain elongation of polyunsaturated fatty acids by vascular endothelial cells: studies with arachidonate analogues. *Lipids.* **25:** 211–215.
96. Rotstein, N. P., and M. I. Aveldano. 1987. Labeling of lipids of retina subcellular fractions by [1–14C]eicosatetraenoate (20:4(n-6)) docosapentaenoate (22:5(n-3)) and docosahexaenoate (22:6(n-3)). *Biochim. Biophys. Acta.* **921:** 221–234.
97. Rotstein, N. P., and M. I. Aveldano. 1987. Labeling of phosphatidylcholines of retina subcellular fractions by [1–14C]eicosatetraenoate (20:4(n-6)), docosapentaenoate (22:5(n-3)) and docosahexaenoate (22:6(n-3)). *Biochim. Biophys. Acta.* **921:** 235–244.
98. Suh, M., and M. T. Clandinin. 2005. 20:5n-3 but not 22:6n-3 is a preferred substrate for synthesis of n-3 very-long- chain fatty acids (C24–C36) in retina. *Curr. Eye Res.* **30:** 959–968.
99. Bazan, H. E., M. M. Careaga, H. Sprecher, and N. G. Bazan. 1982. Chain elongation and desaturation of eicosapentaenoate to docosahexaenoate and phospholipid labeling in the rat retina in vivo. *Biochim. Biophys. Acta.* **712:** 123–128.
100. Wetzel, M. G., J. Li, R. A. Alvarez, R. E. Anderson, and P. J. O'Brien. 1991. Metabolism of linolenic acid and docosahexaenoic acid in rat retinas and rod outer segments. *Exp. Eye Res.* **53:** 437–446.
101. Rotstein, N. P., G. L. Pennacchiotti, H. Sprecher, and M. I. Aveldano. 1996. Active synthesis of C24:5, n-3 fatty acid in retina. *Biochem. J.* **316:** 859–864.
102. Agbaga, M-P. M. Y., S. Logan, R. S. Brush, M. A. Mandal, R. E. Anderson. 2010. ELOVL4 protein elongates n3 and n6 long chain polyunsaturated fatty acids to very long chain polyunsaturated fatty acids. International Society for the Study of Fatty Acids and Lipids (ISSFAL), Maastricht, Netherlands.
103. Smith, S. 1994. The animal fatty acid synthase: one gene, one polypeptide, seven enzymes. *FASEB J.* **8:** 1248–1259.
104. Jakobsson, A., R. Westerberg, and A. Jacobsson. 2006. Fatty acid elongases in mammals: their regulation and roles in metabolism. *Prog. Lipid Res.* **45:** 237–249.
105. Anderson, R. E. 1978. Essential fatty acid deficiency and photoreceptor membrane renewal–a reappraisal. *Invest. Ophthalmol. Vis. Sci.* **17:** 1102–1104.
106. Anderson, R. E., D. J. Landis, and P. A. Dudley. 1976. Essential fatty acid deficiency and renewal of rod outer segments in the albino rat. *Invest. Ophthalmol.* **15:** 232–236.
107. Anderson, R. E., and M. B. Maude. 1972. Lipids of ocular tissues. 8. The effects of essential fatty acid deficiency on the phospholipids of the photoreceptor membranes of rat retina. *Arch. Biochem. Biophys.* **151:** 270–276.
108. Spector, A. A. 1999. Essentiality of fatty acids. *Lipids.* **34 (Suppl.):** S1–S3.
109. Birch, E. E., D. G. Birch, D. R. Hoffman, and R. Uauy. 1992. Dietary essential fatty acid supply and visual acuity development. *Invest. Ophthalmol. Vis. Sci.* **33:** 3242–3253.
110. Connor, W. E., M. Neuringer, and S. Reisbick. 1992. Essential fatty acids: the importance of n-3 fatty acids in the retina and brain. *Nutr. Rev.* **50:** 21–29.
111. Connor, W. E., M. Neuringer, and S. Reisbick. 1991. Essentiality of omega 3 fatty acids: evidence from the primate model and implications for human nutrition. *World Rev. Nutr. Diet.* **66:** 118–132.
112. Neuringer, M., and W. E. Connor. 1986. n-3 fatty acids in the brain and retina: evidence for their essentiality. *Nutr. Rev.* **44:** 285–294.
113. Sprecher, H. 1981. Biochemistry of essential fatty acids. *Prog. Lipid Res.* **20:** 13–22.
114. Bach, L., L. V. Michaelson, R. Haslam, Y. Bellec, L. Gissot, J. Marion, M. Da Costa, J. P. Boutin, M. Miquel, F. Tellier, et al. 2008. The very-long-chain hydroxy fatty acyl-CoA dehydratase PASTICCINO2 is essential and limiting for plant development. *Proc. Natl. Acad. Sci. USA.* **105:** 14727–14731.
115. Paul, S., K. Gable, F. Beaudoin, E. Cahoon, J. Jaworski, J. A. Napier, and T. M. Dunn. 2006. Members of the Arabidopsis FAE1-like 3-ketoacyl-CoA synthase gene family substitute for the Elop proteins of Saccharomyces cerevisiae. *J. Biol. Chem.* **281:** 9018–9029.
116. Beaudoin, F., K. Gable, O. Sayanova, T. Dunn, and J. A. Napier. 2002. A Saccharomyces cerevisiae gene required for heterologous fatty acid elongase activity encodes a microsomal beta-keto-reductase. *J. Biol. Chem.* **277:** 11481–11488.
117. Cinti, D. L., L. Cook, M. N. Nagi, and S. K. Suneja. 1992. The fatty acid chain elongation system of mammalian endoplasmic reticulum. *Prog. Lipid Res.* **31:** 1–51.
118. Zhang, K., M. Kniazeva, M. Han, W. Li, Z. Yu, Z. Yang, Y. Li, M. L. Metzker, R. Allikmets, D. J. Zack, et al. 2001. A 5-bp deletion in ELOVL4 is associated with two related forms of autosomal dominant macular dystrophy. *Nat. Genet.* **27:** 89–93.
119. Fritzler, J. M., J. J. Millership, and G. Zhu. 2007. Cryptosporidium parvum long-chain fatty acid elongase. *Eukaryot. Cell.* **6:** 2018–2028.
120. Bernert, J. T., Jr., and H. Sprecher. 1977. An analysis of partial reactions in the overall chain elongation of saturated and unsaturated fatty acids by rat liver microsomes. *J. Biol. Chem.* **252:** 6736–6744.
121. Nugteren, D. H. 1965. The enzymic chain elongation of fatty acids by rat-liver microsomes. *Biochim. Biophys. Acta.* **106:** 280–290.
122. Leonard, A. E., S. L. Pereira, H. Sprecher, and Y. S. Huang. 2004. Elongation of long-chain fatty acids. *Prog. Lipid Res.* **43:** 36–54.
123. Kang, Z. B., Y. Ge, Z. Chen, J. Cluette-Brown, M. Laposata, A. Leaf, and J. X. Kang. 2001. Adenoviral gene transfer of Caenorhabditis elegans n–3 fatty acid desaturase optimizes fatty acid composition in mammalian cells. *Proc. Natl. Acad. Sci. USA.* **98:** 4050–4054.
124. Meyer, A., H. Kirsch, F. Domergue, A. Abbadi, P. Sperling, J. Bauer, P. Cirpus, T. K. Zank, H. Moreau, T. J. Roscoe, et al. 2004. Novel fatty acid elongases and their use for the reconstitution of docosahexaenoic acid biosynthesis. *J. Lipid Res.* **45:** 1899–1909.
125. Westerberg, R., P. Tvrdik, A. B. Unden, J. E. Mansson, L. Norlen, A. Jakobsson, W. H. Holleran, P. M. Elias, A. Asadi, P. Flodby, et al. 2004. Role for ELOVL3 and fatty acid chain length in development of hair and skin function. *J. Biol. Chem.* **279:** 5621–5629.
126. Abbadi, A., F. Domergue, J. Bauer, J. A. Napier, R. Welti, U. Zahringer, P. Cirpus, and E. Heinz. 2004. Biosynthesis of very-long-chain polyunsaturated fatty acids in transgenic oilseeds: constraints on their accumulation. *Plant Cell.* **16:** 2734–2748.
127. Napier, J. A., F. Beaudoin, L. V. Michaelson, and O. Sayanova. 2004. The production of long chain polyunsaturated fatty acids in transgenic plants by reverse-engineering. *Biochimie.* **86:** 785–792.
128. Toke, D. A., and C. E. Martin. 1996. Isolation and characterization of a gene affecting fatty acid elongation in Saccharomyces cerevisiae. *J. Biol. Chem.* **271:** 18413–18422.
129. Dittrich, F., D. Zajonc, K. Huhne, U. Hoja, A. Ekici, E. Greiner, H. Klein, J. Hofmann, J. J. Bessoule, P. Sperling, et al. 1998. Fatty acid elongation in yeast–biochemical characteristics of the enzyme system and isolation of elongation-defective mutants. *Eur. J. Biochem.* **252:** 477–485.
130. Moon, Y. A., N. A. Shah, S. Mohapatra, J. A. Warrington, and J. D. Horton. 2001. Identification of a mammalian long chain fatty acyl elongase regulated by sterol regulatory element-binding proteins. *J. Biol. Chem.* **276:** 45358–45366.

131. David, D., S. Sundarababu, and J. E. Gerst. 1998. Involvement of long chain fatty acid elongation in the trafficking of secretory vesicles in yeast. *J. Cell Biol.* **143:** 1167–1182.
132. Tvrdik, P., A. Asadi, L. P. Kozak, J. Nedergaard, B. Cannon, and A. Jacobsson. 1997. Cig30, a mouse member of a novel membrane protein gene family, is involved in the recruitment of brown adipose tissue. *J. Biol. Chem.* **272:** 31738–31746.
133. Tvrdik, P., R. Westerberg, S. Silve, A. Asadi, A. Jakobsson, B. Cannon, G. Loison, and A. Jacobsson. 2000. Role of a new mammalian gene family in the biosynthesis of very long chain fatty acids and sphingolipids. *J. Cell Biol.* **149:** 707–718.
134. Jakobsson, A., J. A. Jorgensen, and A. Jacobsson. 2005. Differential regulation of fatty acid elongation enzymes in brown adipocytes implies a unique role for Elovl3 during increased fatty acid oxidation. *Am. J. Physiol. Endocrinol. Metab.* **289:** E517–E526.
135. Westerberg, R., J. E. Mansson, V. Golozoubova, I. G. Shabalina, E. C. Backlund, P. Tvrdik, K. Retterstol, M. R. Capecchi, and A. Jacobsson. 2006. ELOVL3 is an important component for early onset of lipid recruitment in brown adipose tissue. *J. Biol. Chem.* **281:** 4958–4968.
136. Ofman, R., I. M. Dijkstra, C. W. van Roermund, N. Burger, M. Turkenburg, A. van Cruchten, C. E. van Engen, R. J. Wanders, and S. Kemp. 2010. The role of ELOVL1 in very long-chain fatty acid homeostasis and X-linked adrenoleukodystrophy. *EMBO Mol. Med.* **2:** 90–97.
137. Bourre, J. M., M. Y. Paturneau-Jouas, O. L. Daudu, and N. A. Baumann. 1977. Lignoceric acid biosynthesis in the developing brain. Activities of mitochondrial acetyl- CoA-dependent synthesis and microsomal malonyl-CoA chain-elongating system in relation to myelination. Comparison between normal mouse and dysmyelinating mutants (quaking and jimpy). *Eur. J. Biochem.* **72:** 41–47.
138. Leonard, A. E., E. G. Bobik, J. Dorado, P. E. Kroeger, L. T. Chuang, J. M. Thurmond, J. M. Parker-Barnes, T. Das, Y. S. Huang, and P. Mukerji. 2000. Cloning of a human cDNA encoding a novel enzyme involved in the elongation of long-chain polyunsaturated fatty acids. *Biochem. J.* **350:** 765–770.
139. Leonard, A. E., B. Kelder, E. G. Bobik, L. T. Chuang, C. J. Lewis, J. J. Kopchick, P. Mukerji, and Y. S. Huang. 2002. Identification and expression of mammalian long- chain PUFA elongation enzymes. *Lipids.* **37:** 733–740.
140. Bernstein, P. S., J. Tammur, N. Singh, A. Hutchinson, M. Dixon, C. M. Pappas, N. A. Zabriskie, K. Zhang, K. Petrukhin, M. Leppert, et al. 2001. Diverse macular dystrophy phenotype caused by a novel complex mutation in the ELOVL4 gene. *Invest. Ophthalmol. Vis. Sci.* **42:** 3331–3336.
141. Edwards, A. O., L. A. Donoso, and R. Ritter 3rd. 2001. A novel gene for autosomal dominant Stargardt-like macular dystrophy with homology to the SUR4 protein family. *Invest. Ophthalmol. Vis. Sci.* **42:** 2652–2663.
142. Bedell, M., R. Harkewicz, X. Wang, and K. Zhang. 2010. Focus on molecules: ELOVL4. *Exp. Eye Res.* **90:** 476–477.
143. Vasireddy, V., P. Wong, and R. Ayyagari. 2010. Genetics and molecular pathology of Stargardt-like macular degeneration. *Prog. Retin. Eye Res.* **29:** 191–207.
144. Inagaki, K., T. Aki, Y. Fukuda, S. Kawamoto, S. Shigeta, K. Ono, and O. Suzuki. 2002. Identification and expression of a rat fatty acid elongase involved in the biosynthesis of C18 fatty acids. *Biosci. Biotechnol. Biochem.* **66:** 613–621.
145. Wang, Y., M. Torres-Gonzalez, S. Tripathy, D. Botolin, B. Christian, and D. B. Jump. 2008. Elevated hepatic fatty acid elongase-5 activity affects multiple pathways controlling hepatic lipid and carbohydrate composition. *J. Lipid Res.* **49:** 1538–1552.
146. Moon, Y. A., R. E. Hammer, and J. D. Horton. 2009. Deletion of ELOVL5 leads to fatty liver through activation of SREBP-1c in mice. *J. Lipid Res.* **50:** 412–423.
147. Tamura, K., A. Makino, F. Hullin-Matsuda, T. Kobayashi, M. Furihata, S. Chung, S. Ashida, T. Miki, T. Fujioka, T. Shuin, et al. 2009. Novel lipogenic enzyme ELOVL7 is involved in prostate cancer growth through saturated long-chain fatty acid metabolism. *Cancer Res.* **69:** 8133–8140.
148. Tikhonenko, M., T. A. Lydic, Y. Wang, W. Chen, M. Opreanu, A. Sochacki, K. M. McSorley, R. L. Renis, T. Kern, D. B. Jump, et al. 2010. Remodeling of retinal fatty acids in an animal model of diabetes: a decrease in long chain polyunsaturated fatty acids is associated with a decrease in fatty acid elongases Elovl2 and Elovl4. *Diabetes.* **59:** 219–227.
149. Mandal, M. N., R. Ambasudhan, P. W. Wong, P. J. Gage, P. A. Sieving, and R. Ayyagari. 2004. Characterization of mouse orthologue of ELOVL4: genomic organization and spatial and temporal expression. *Genomics.* **83:** 626–635.
150. Lagali, P. S., I. M. MacDonald, I. B. Griesinger, M. L. Chambers, R. Ayyagari, and P. W. Wong. 2000. Autosomal dominant Stargardt-like macular dystrophy segregating in a large Canadian family. *Can. J. Ophthalmol.* **35:** 315–324.
151. Griesinger, I. B., P. A. Sieving, and R. Ayyagari. 2000. Autosomal dominant macular atrophy at 6q14 excludes CORD7 and MCDR1/PBCRA loci. *Invest. Ophthalmol. Vis. Sci.* **41:** 248–255.
152. Ambasudhan, R., X. Wang, M. M. Jablonski, D. A. Thompson, P. S. Lagali, P. W. Wong, P. A. Sieving, and R. Ayyagari. 2004. Atrophic macular degeneration mutations in ELOVL4 result in the intracellular misrouting of the protein. *Genomics.* **83:** 615–625.
153. Donoso, L. A., A. O. Edwards, A. Frost, T. Vrabec, E. M. Stone, G. S. Hageman, and T. Perski. 2001. Autosomal dominant Stargardt-like macular dystrophy. *Surv. Ophthalmol.* **46:** 149–163.
154. Michaelides, M., D. M. Hunt, and A. T. Moore. 2003. The genetics of inherited macular dystrophies. *J. Med. Genet.* **40:** 641–650.
155. Edwards, A. O., A. Miedziak, T. Vrabec, J. Verhoeven, T. S. Acott, R. G. Weleber, and L. A. Donoso. 1999. Autosomal dominant Stargardt-like macular dystrophy. I. Clinical characterization, longitudinal follow-up, and evidence for a common ancestry in families linked to chromosome 6q14. *Am. J. Ophthalmol.* **127:** 426–435.
156. Stone, E. M., B. E. Nichols, A. E. Kimura, T. A. Weingeist, A. Drack, and V. C. Sheffield. 1994. Clinical features of a Stargardt-like dominant progressive macular dystrophy with genetic linkage to chromosome 6q. *Arch. Ophthalmol.* **112:** 765–772.
157. Kniazeva, M., M. F. Chiang, B. Morgan, A. L. Anduze, D. J. Zack, M. Han, and K. Zhang. 1999. A new locus for autosomal dominant stargardt-like disease maps to chromosome 4. *Am. J. Hum. Genet.* **64:** 1394–1399.
158. Bither, P. P., and L. A. Berns. 1988. Dominant inheritance of Stargardt's disease. *J. Am. Optom. Assoc.* **59:** 112–117.
159. Zhang, K., P. P. Bither, R. Park, L. A. Donoso, J. G. Seidman, and C. E. Seidman. 1994. A dominant Stargardt's macular dystrophy locus maps to chromosome 13q34. *Arch. Ophthalmol.* **112:** 759–764.
160. Maugeri, A., F. Meire, C. B. Hoyng, C. Vink, N. Van Regemorter, G. Karan, Z. Yang, F. P. Cremers, and K. Zhang. 2004. A novel mutation in the ELOVL4 gene causes autosomal dominant Stargardt-like macular dystrophy. *Invest. Ophthalmol. Vis. Sci.* **45:** 4263–4267.
161. Zhang, X. M., Z. Yang, G. Karan, T. Hashimoto, W. Baehr, X. J. Yang, and K. Zhang. 2003. Elovl4 mRNA distribution in the developing mouse retina and phylogenetic conservation of Elovl4 genes. *Mol. Vis.* **9:** 301–307.
162. Lagali, P. S., J. Liu, R. Ambasudhan, L. E. Kakuk, S. L. Bernstein, G. M. Seigel, P. W. Wong, and R. Ayyagari. 2003. Evolutionarily conserved ELOVL4 gene expression in the vertebrate retina. *Invest. Ophthalmol. Vis. Sci.* **44:** 2841–2850.
163. Grayson, C., and R. S. Molday. 2005. Dominant negative mechanism underlies autosomal dominant Stargardt-like macular dystrophy linked to mutations in ELOVL4. *J. Biol. Chem.* **280:** 32521–32530.
164. Umeda, S., R. Ayyagari, M. T. Suzuki, F. Ono, F. Iwata, K. Fujiki, A. Kanai, Y. Takada, Y. Yoshikawa, Y. Tanaka, et al. 2003. Molecular cloning of ELOVL4 gene from cynomolgus monkey (Macaca fascicularis). *Exp. Anim.* **52:** 129–135.
165. Karan, G., C. Lillo, Z. Yang, D. J. Cameron, K. G. Locke, Y. Zhao, S. Thirumalaichary, C. Li, D. G. Birch, H. R. Vollmer-Snarr, et al. 2005. Lipofuscin accumulation, abnormal electrophysiology, and photoreceptor degeneration in mutant ELOVL4 transgenic mice: a model for macular degeneration. *Proc. Natl. Acad. Sci. USA.* **102:** 4164–4169.
166. Li, W., Y. Chen, D. J. Cameron, C. Wang, G. Karan, Z. Yang, Y. Zhao, E. Pearson, H. Chen, C. Deng, et al. 2007. Elovl4 haploinsufficiency does not induce early onset retinal degeneration in mice. *Vision Res.* **47:** 714–722.
167. Raz-Prag, D., R. Ayyagari, R. N. Fariss, M. N. Mandal, V. Vasireddy, S. Majchrzak, A. L. Webber, R. A. Bush, N. Salem, Jr., K. Petrukhin, et al. 2006. Haploinsufficiency is not the key mechanism of pathogenesis in a heterozygous Elovl4 knockout mouse model of STGD3 disease. *Invest. Ophthalmol. Vis. Sci.* **47:** 3603–3611.
168. Vasireddy, V., M. M. Jablonski, M. N. Mandal, D. Raz-Prag, X. F. Wang, L. Nizol, A. Iannaccone, D. C. Musch, R. A. Bush, N. Salem, Jr., et al. 2006. Elovl4 5-bp-deletion knock-in mice develop

progressive photoreceptor degeneration. *Invest. Ophthalmol. Vis. Sci.* **47:** 4558–4568.
169. Street, J. M., D. W. Johnson, H. Singh, and A. Poulos. 1989. Metabolism of saturated and polyunsaturated fatty acids by normal and Zellweger syndrome skin fibroblasts. *Biochem. J.* **260:** 647–655.
170. Uchida, Y., and W. M. Holleran. 2008. Omega-O-acylceramide, a lipid essential for mammalian survival. *J. Dermatol. Sci.* **51:** 77–87.
171. McMahon, A. I. A. B., S. N. Jackson, X. Liu, M. Klein, D. G. Birch, A. Woods, and W. Kedzierski. 2010. Generation of Homozygous Stargardt-3 Mice Which Completely Lack Retinal Polyunsaturated C28–C36 Fatty Acids. The Association for Research in Vision and Ophthalmology, Fort Lauderdale, FL.
172. Kedzierski, W. X. L., M. Klein, S.N. Jackson, I. Butovich, D. Birch, A. Woods, and A. McMahon. 2010. Abnormal Retinal Morphology and Function in Homozygous Stargardt-3 Mice Which Completely Lack Polyunsaturated C28–C36 Fatty Acids in the Mature Retina. The Association for Research in Vision and Ophthalmology, Fort Lauderdale, FL.
173. Karan, G., Z. Yang, K. Howes, Y. Zhao, Y. Chen, D. J. Cameron, Y. Lin, E. Pearson, and K. Zhang. 2005. Loss of ER retention and sequestration of the wild-type ELOVL4 by Stargardt disease dominant negative mutants. *Mol. Vis.* **11:** 657–664.
174. Karan, G., Z. Yang, and K. Zhang. 2004. Expression of wild type and mutant ELOVL4 in cell culture: subcellular localization and cell viability. *Mol. Vis.* **10:** 248–253.
175. Vasireddy, V., C. Vijayasarathy, J. Huang, X. F. Wang, M. M. Jablonski, H. R. Petty, P. A. Sieving, and R. Ayyagari. 2005. Stargardt-like macular dystrophy protein ELOVL4 exerts a dominant negative effect by recruiting wild-type protein into aggresomes. *Mol. Vis.* **11:** 665–676.
176. Li, F., L. D. Marchette, R. S. Brush, M. H. Elliott, Y. Z. Le, K. A. Henry, A. G. Anderson, C. Zhao, X. Sun, K. Zhang, et al. 2009. DHA does not protect ELOVL4 transgenic mice from retinal degeneration. *Mol. Vis.* **15:** 1185–1193.
177. Kang, J. X. 2007. Fat-1 transgenic mice: a new model for omega-3 research. *Prostaglandins Leukot. Essent. Fatty Acids.* **77:** 263–267.
178. Kang, J. X., J. Wang, L. Wu, and Z. B. Kang. 2004. Transgenic mice: fat-1 mice convert n-6 to n-3 fatty acids. *Nature.* **427:** 504.
179. Bloomston, M., A. Durkin, I. Yang, M. Rojiani, A. S. Rosemurgy, S. Enkmann, T. J. Yeatman, and E. E. Zervos. 2004. Identification of molecular markers specific for pancreatic neuroendocrine tumors by genetic profiling of core biopsies. *Ann. Surg. Oncol.* **11:** 413–419.
180. Omura, N., C. P. Li, A. Li, S. M. Hong, K. Walter, A. Jimeno, M. Hidalgo, and M. Goggins. 2008. Genome-wide profiling of methylated promoters in pancreatic adenocarcinoma. *Cancer Biol. Ther.* **7:** 1146–1156.
181. Barqawi, A., H. Trummer, and R. Meacham. 2004. Effect of prolonged cryptorchidism on germ cell apoptosis and testicular sperm count. *Asian J. Androl.* **6:** 47–51.
182. Farooqui, S. M., F. Al-Bagdadi, J. M. O'Donnell, and R. Stout. 1997. Degenerative changes in spermatogonia are associated with loss of glucose transporter (Glut 3) in abdominal testis of surgically induced unilateral cryptorchidism in rats. *Biochem. Biophys. Res. Commun.* **236:** 407–412.
183. Zanetti, S. R., E. N. Maldonado, and M. I. Aveldano. 2007. Doxorubicin affects testicular lipids with long-chain (C18–C22) and very long-chain (C24–C32) polyunsaturated fatty acids. *Cancer Res.* **67:** 6973–6980.
184. Stoffel, W., B. Holz, B. Jenke, E. Binczek, R. H. Gunter, C. Kiss, I. Karakesisoglou, M. Thevis, A. A. Weber, S. Arnhold, et al. 2008. Delta 6-desaturase (FADS2) deficiency unveils the role of omega 3- and omega 6-polyunsaturated fatty acids. *EMBO J.* **27:** 2281–2292.
185. Roqueta-Rivera, M., C. K. Stroud, W. M. Haschek, S. J. Akare, M. Segre, R. S. Brush, M. P. Agbaga, R. E. Anderson, R. A. Hess, and M. T. Nakamura. 2010. Docosahexaenoic acid supplementation fully restores fertility and spermatogenesis in male delta-6 desaturase-null mice. *J. Lipid Res.* **51:** 360–367.
186. Anderson, R. E. 1982. Renewal of lipids in rod outer segments. *Methods Enzymol.* **81:** 800–806.
187. Anderson, R. E., R. M. Benolken, P. A. Dudley, D. J. Landis, and T. G. Wheeler. 1974. Proceedings: Polyunsaturated fatty acids of photoreceptor membranes. *Exp. Eye Res.* **18:** 205–213.
188. James, M. J., R. A. Gibson, and L. G. Cleland. 2000. Dietary polyunsaturated fatty acids and inflammatory mediator production. *Am. J. Clin. Nutr.* **71:** 343S–348S.
189. Bazan, N. G., and G. Allan. 1997. Signal transduction and gene expression in the eye: a contemporary view of the pro-inflammatory, anti-inflammatory and modulatory roles of prostaglandins and other bioactive lipids. *Surv. Ophthalmol.* **41 (Suppl. 2):** S23–S34.
190. Watts, J. L., and J. Browse. 2002. Genetic dissection of polyunsaturated fatty acid synthesis in Caenorhabditis elegans. *Proc. Natl. Acad. Sci. USA.* **99:** 5854–5859.
191. Xiao, Y. F., Q. Ke, S. Y. Wang, K. Auktor, Y. Yang, G. K. Wang, J. P. Morgan, and A. Leaf. 2001. Single point mutations affect fatty acid block of human myocardial sodium channel alpha subunit Na+ channels. *Proc. Natl. Acad. Sci. USA.* **98:** 3606–3611.
192. Chyb, S., P. Raghu, and R. C. Hardie. 1999. Polyunsaturated fatty acids activate the Drosophila light-sensitive channels TRP and TRPL. *Nature.* **397:** 255–259.
193. Litman, B. J., S. L. Niu, A. Polozova, and D. C. Mitchell. 2001. The role of docosahexaenoic acid containing phospholipids in modulating G protein-coupled signaling pathways: visual transduction. *J. Mol. Neurosci.* **16:** 237–242, discussion 279–284.
194. Mitchell, D. C., S. L. Niu, and B. J. Litman. 2001. Optimization of receptor-G protein coupling by bilayer lipid composition I: kinetics of rhodopsin-transducin binding. *J. Biol. Chem.* **276:** 42801–42806.
195. Niu, S. L., D. C. Mitchell, and B. J. Litman. 2001. Optimization of receptor-G protein coupling by bilayer lipid composition II: formation of metarhodopsin II-transducin complex. *J. Biol. Chem.* **276:** 42807–42811.
196. Mitchell, D. C., S. L. Niu, and B. J. Litman. 2003. DHA-rich phospholipids optimize G-Protein-coupled signaling. *J. Pediatr.* **143:** S80–S86.
197. Mitchell, D. C., S. L. Niu, and B. J. Litman. 2003. Enhancement of G protein-coupled signaling by DHA phospholipids. *Lipids.* **38:** 437–443.
198. Crawford, M. A., K. Costeloe, K. Ghebremeskel, A. Phylactos, L. Skirvin, and F. Stacey. 1997. Are deficits of arachidonic and docosahexaenoic acids responsible for the neural and vascular complications of preterm babies? *Am. J. Clin. Nutr.* **66:** 1032S–1041S.
199. Salem, N., Jr., B. Wegher, P. Mena, and R. Uauy. 1996. Arachidonic and docosahexaenoic acids are biosynthesized from their 18-carbon precursors in human infants. *Proc. Natl. Acad. Sci. USA.* **93:** 49–54.
200. Uauy, R., P. Peirano, D. Hoffman, P. Mena, D. Birch, and E. Birch. 1996. Role of essential fatty acids in the function of the developing nervous system. *Lipids.* **31 (Suppl.):** S167–S176.
201. Bazan, N. G. 2008. Neuroprotectin D1-mediated anti-inflammatory and survival signaling in stroke, retinal degenerations and Alzheimer's disease. *J. Lipid Res.* **50 (Suppl.):** S400–S405.
202. Mukherjee, P. K., V. L. Marcheselli, C. N. Serhan, and N. G. Bazan. 2004. Neuroprotectin D1: a docosahexaenoic acid-derived docosatriene protects human retinal pigment epithelial cells from oxidative stress. *Proc. Natl. Acad. Sci. USA.* **101:** 8491–8496.
203. Ramstedt, B., and J. P. Slotte. 1999. Interaction of cholesterol with sphingomyelins and acyl-chain-matched phosphatidylcholines: a comparative study of the effect of the chain length. *Biophys. J.* **76:** 908–915.
204. Janmey, P. A., and P. K. Kinnunen. 2006. Biophysical properties of lipids and dynamic membranes. *Trends Cell Biol.* **16:** 538–546.
205. Szafer-Glusman, E., M. G. Giansanti, R. Nishihama, B. Bolival, J. Pringle, M. Gatti, and M. T. Fuller. 2008. A role for very-long-chain fatty acids in furrow ingression during cytokinesis in Drosophila spermatocytes. *Curr. Biol.* **18:** 1426–1431.
206. Aveldano, M. I. 1988. Phospholipid species containing long and very long polyenoic fatty acids remain with rhodopsin after hexane extraction of photoreceptor membranes. *Biochemistry.* **27:** 1229–1239.
207. Li, J., P. C. Edwards, M. Burghammer, C. Villa, and G. F. Schertler. 2004. Structure of bovine rhodopsin in a trigonal crystal form. *J. Mol. Biol.* **343:** 1409–1438.
208. Brown, M. F. 1994. Modulation of rhodopsin function by properties of the membrane bilayer. *Chem. Phys. Lipids.* **73:** 159–180.
209. Niu, S. L., D. C. Mitchell, S. Y. Lim, Z. M. Wen, H. Y. Kim, N. Salem, Jr., and B. J. Litman. 2004. Reduced G protein-coupled signaling efficiency in retinal rod outer segments in response to n-3 fatty acid deficiency. *J. Biol. Chem.* **279:** 31098–31104.
210. Gawrisch, K., and O. Soubias. 2008. Structure and dynamics of polyunsaturated hydrocarbon chains in lipid bilayers-significance for GPCR function. *Chem. Phys. Lipids.* **153:** 64–75.
211. Gawrisch, K., O. Soubias, and M. Mihailescu. 2008. Insights from biophysical studies on the role of polyunsaturated fatty acids for

function of G-protein coupled membrane receptors. *Prostaglandins Leukot. Essent. Fatty Acids.* **79:** 131–134.
212. Grossfield, A., M. C. Pitman, S. E. Feller, O. Soubias, and K. Gawrisch. 2008. Internal hydration increases during activation of the G-protein-coupled receptor rhodopsin. *J. Mol. Biol.* **381:** 478–486.
213. Soubias, O., and K. Gawrisch. 2005. Probing specific lipid-protein interaction by saturation transfer difference NMR spectroscopy. *J. Am. Chem. Soc.* **127:** 13110–13111.
214. Denic, V., and J. S. Weissman. 2007. A molecular caliper mechanism for determining very long-chain fatty acid length. *Cell.* **130:** 663–677.
215. Contreras, F. X., G. Basanez, A. Alonso, A. Herrmann, and F. M. Goni. 2005. Asymmetric addition of ceramides but not dihydroceramides promotes transbilayer (flip-flop) lipid motion in membranes. *Biophys. J.* **88:** 348–359.
216. Schneiter, R., B. Brugger, C. M. Amann, G. D. Prestwich, R. F. Epand, G. Zellnig, F. T. Wieland, and R. M. Epand. 2004. Identification and biophysical characterization of a very-long-chain-fatty-acid-substituted phosphatidylinositol in yeast subcellular membranes. *Biochem. J.* **381:** 941–949.
217. Beharry, S., M. Zhong, and R. S. Molday. 2004. N-retinylidene-phosphatidylethanolamine is the preferred retinoid substrate for the photoreceptor- specific ABC transporter ABCA4 (ABCR). *J. Biol. Chem.* **279:** 53972–53979.
218. Weng, J., N. L. Mata, S. M. Azarian, R. T. Tzekov, D. G. Birch, and G. H. Travis. 1999. Insights into the function of Rim protein in photoreceptors and etiology of Stargardt's disease from the phenotype in abcr knockout mice. *Cell.* **98:** 13–23.
219. Allikmets, R., N. F. Shroyer, N. Singh, J. M. Seddon, R. A. Lewis, P. S. Bernstein, A. Peiffer, N. A. Zabriskie, Y. Li, A. Hutchinson, et al. 1997. Mutation of the Stargardt disease gene (ABCR) in age-related macular degeneration. *Science.* **277:** 1805–1807.
220. Allikmets, R., N. Singh, H. Sun, N. F. Shroyer, A. Hutchinson, A. Chidambaram, B. Gerrard, L. Baird, D. Stauffer, A. Peiffer, et al. 1997. A photoreceptor cell-specific ATP-binding transporter gene (ABCR) is mutated in recessive Stargardt macular dystrophy. *Nat. Genet.* **15:** 236–246.
221. Zhang, K., M. Kniazeva, A. Hutchinson, M. Han, M. Dean, and R. Allikmets. 1999. The ABCR gene in recessive and dominant Stargardt diseases: a genetic pathway in macular degeneration. *Genomics.* **60:** 234–237.
222. Maugeri, A., B. J. Klevering, K. Rohrschneider, A. Blankenagel, H. G. Brunner, A. F. Deutman, C. B. Hoyng, and F. P. Cremers. 2000. Mutations in the ABCA4 (ABCR) gene are the major cause of autosomal recessive cone-rod dystrophy. *Am. J. Hum. Genet.* **67:** 960–966.
223. Zhang, K., D. C. Garibaldi, M. Kniazeva, T. Albini, M. F. Chiang, M. Kerrigan, J. S. Sunness, M. Han, and R. Allikmets. 1999. A novel mutation in the ABCR gene in four patients with autosomal recessive Stargardt disease. *Am. J. Ophthalmol.* **128:** 720–724.
224. Vasireddy, V., M. M. Jablonski, N. W. Khan, X. F. Wang, P. Sahu, J. R. Sparrow, and R. Ayyagari. 2009. Elovl4 5-bp deletion knock-in mouse model for Stargardt-like macular degeneration demonstrates accumulation of ELOVL4 and lipofuscin. *Exp. Eye Res.* **89:** 905–912.
225. Mata, N. L., J. Weng, and G. H. Travis. 2000. Biosynthesis of a major lipofuscin fluorophore in mice and humans with ABCR-mediated retinal and macular degeneration. *Proc. Natl. Acad. Sci. USA.* **97:** 7154–7159.
226. Birch, D. G., and J. L. Anderson. 1992. Standardized full-field electroretinography. Normal values and their variation with age. *Arch. Ophthalmol.* **110:** 1571–1576.
227. Weleber, R. G. 1981. The effect of age on human cone and rod ganzfeld electroretinograms. *Invest. Ophthalmol. Vis. Sci.* **20:** 392–399.
228. Li, C., M. Cheng, H. Yang, N. S. Peachey, and M. I. Naash. 2001. Age-related changes in the mouse outer retina. *Optom. Vis. Sci.* **78:** 425–430.
229. Benolken, R. M., R. E. Anderson, and T. G. Wheeler. 1973. Membrane fatty acids associated with the electrical response in visual excitation. *Science.* **182:** 1253–1254.
230. Landis, D. J., P. A. Dudley, and R. E. Anderson. 1973. Alteration of disc formation in photoreceptors of rat retina. *Science.* **182:** 1144–1146.
231. Jeffrey, B. G., D. C. Mitchell, R. A. Gibson, and M. Neuringer. 2002. n-3 fatty acid deficiency alters recovery of the rod photoresponse in rhesus monkeys. *Invest. Ophthalmol. Vis. Sci.* **43:** 2806–2814.
232. Litman, B. J., and D. C. Mitchell. 1996. A role for phospholipid polyunsaturation in modulating membrane protein function. *Lipids.* **31 (Suppl.):** S193–S197.
233. Neuringer, M., W. E. Connor, D. S. Lin, L. Barstad, and S. Luck. 1986. Biochemical and functional effects of prenatal and postnatal omega 3 fatty acid deficiency on retina and brain in rhesus monkeys. *Proc. Natl. Acad. Sci. USA.* **83:** 4021–4025.
234. Neuringer, M., W. E. Connor, C. Van Petten, and L. Barstad. 1984. Dietary omega-3 fatty acid deficiency and visual loss in infant rhesus monkeys. *J. Clin. Invest.* **73:** 272–276.
235. Neuringer, M., S. Reisbick, and J. Janowsky. 1994. The role of n-3 fatty acids in visual and cognitive development: current evidence and methods of assessment. *J. Pediatr.* **125:** S39–S47.
236. Shaikh, S. R., and M. Edidin. 2006. Polyunsaturated fatty acids, membrane organization, T cells, and antigen presentation. *Am. J. Clin. Nutr.* **84:** 1277–1289.
237. Stulnig, T. M. 2003. Immunomodulation by polyunsaturated fatty acids: mechanisms and effects. *Int. Arch. Allergy Immunol.* **132:** 310–321.
238. Mazelova, J., N. Ransom, L. Astuto-Gribble, M. C. Wilson, and D. Deretic. 2009. Syntaxin 3 and SNAP-25 pairing, regulated by omega-3 docosahexaenoic acid, controls the delivery of rhodopsin for the biogenesis of cilia-derived sensory organelles, the rod outer segments. *J. Cell Sci.* **122:** 2003–2013.
239. Bazan, N. G. 2008. Neurotrophins induce neuroprotective signaling in the retinal pigment epithelial cell by activating the synthesis of the anti-inflammatory and anti- apoptotic neuroprotectin D1. *Adv. Exp. Med. Biol.* **613:** 39–44.
240. Bazan, N. G. 2005. Neuroprotectin D1 (NPD1): a DHA-derived mediator that protects brain and retina against cell injury-induced oxidative stress. *Brain Pathol.* **15:** 159–166.